X-643-67-535

RESONANT GRAVITY HARMONICS FROM 3-1/2 YEARS OF TRACKING DATA ON THREE 24 HOUR SATELLITES

Carl A. Wagner
Special Projects Branch
Laboratory for Theoretical Studies

November 1967

Goddard Space Flight Center
Greenbelt, Maryland

RESONANT GRAVITY HARMONICS FROM 3-1/2 YEARS OF TRACKING DATA ON THREE 24 HOUR SATELLITES

Carl A. Wagner

ABSTRACT

Over 500 orbits of the synchronous satellites Syncom 2, Syncom 3 and "Early Bird" have been examined to reveal the long term effects of the longitude dependence of the earth's gravitational field. The period of record extends from August 1963 to January 1967. The east-west drift of these synchronous orbits are strongly influenced by the low order gravity harmonics H_{22} and H_{33} which are in resonance with them. The record shows these harmonics to have the following amplitudes and phase angles: $10^6 J_{22} = 1.80 \pm .04$, $\lambda_{22} = -15.3 \pm 0.6°$, $10^6 J_{33} = 0.16 {}^{+0.05}_{-0.03}$, $\lambda_{33} = 26.4 {}^{+6.6°}_{-8.3°}$. The record also shows, but less significantly, the influence of the resonant harmonic H_{31}. The amplitude and phase of this harmonic is found to be: $10^6 J_{31} = 1.5 {}^{+2.6}_{-1.2}$, $\lambda_{31} = -79 {}^{+73°}_{-88°}$. The bounds on these harmonic parameters are felt to be quite conservative and reflect likely effects of higher order resonant gravity harmonics which could not be well determined by the data. The full record through January 1967 now permits the discrimination of the long term east-west drift acceleration of a geostationary satellite to within 5.5×10^{-5} deg/day^2 (Maximum 1σ) around the equator.

CONTENTS

RESONANT GRAVITY HARMONICS FROM 3-1/2 YEARS OF TRACKING DATA ON THREE 24 HOUR SATELLITES

INTRODUCTION

Since July 1963 the National Aeronautics and Space Administration (NASA) and the Communications Satellite Corporation (COMSAT), and the Department of Defense (DOD) have tracked and operated eight synchronous (24 hour) satellites positioned at a fair number of longitudes around the equator. The free drift tracking record of three of these satellites (NASA's Syncoms 2 and 3 and COMSAT's "Early Bird") prior to July 1965 has already revealed new and accurate information about the longitude dependence of the earth's gravity field[1,2]. The lowest or 2nd order longitude components of the field dominate the libratory east-west gravity drift of 24 hour satellites and can cause accelerations as high as 1.9×10^{-3} degrees per day.[2] In order to be able to predict accurately their behavior at all longitudes, good tracking information must be obtained over as wide a longitude range as possible. This is true principally because third and fourth order components of the longitude gravity field have small but significant long term effects on these satellites. These effects can only be accounted for adequately by a wide longitude survey of synchronous satellite drift. This report brings the available tracking record of Syncom 3 and Early Bird up to January 1967. It covers completely the longitude range of these satellites prior to that date. Complete tracking data on Syncom 2 from July 1963 up to April 1966 is also recorded here. Data on this satellite during the rest of 1966 adds about 6 degrees of longitude to this survey. It will be incorporated in future reports on 24 hour satellite drift which will also include the record of the NASA and COMSAT 24 hour satellites ("INTELSAT" and "ATS") launched since December 1966.

The tracking data presented in this report is analyzed for long term east-west drift acceleration according to the methods developed in previous investigations by the author[3,4]. The measured accelerations are then used to solve for specific longitude dependent gravity terms in the earth's potential which can give rise to these perturbations. The essential point of this analysis is that the critical longitude gravity forces are in librational resonance on these satellites. The libration period due to the strongest effect is not less than 2 years. Thus the detailed tracking information taken over a few days, that is summarized by a set of 6 orbital parameters, is probably not much more valuable than the 6 elements themselves in determining the disturbing field. Whenever small perturbation forces give rise to large long term effects, such as the orbital regression and precession due to the oblate earth, the most economical analysis for those forces deals directly with the derived orbital elements themselves as the observed data [5,6]. The satellite's equator crossing longitude, while not a typical orbital element, is easily derived from the set of 6 that are generally given.

The operators of 24 hour satellites are concerned mostly with the drift accelerations which can be expected around the equator. These are finally estimated through the disturbing earth potential derived from the set of observed drift accelerations on the synchronous satellites. The ultimate aim of this report as in the previous one[4], is to give realistic estimates of both the total acceleration and the individual gravity terms affecting the 24 hour satellites.

ANALYSIS AND DATA REDUCTION

The Earth's gravitational potential which is employed in the data analysis is the familiar spherical harmonic expansion in associated Legendre functions ($P_{\ell m}$):

$$V = \frac{\mu}{r}\left[1 + \sum_{\ell=2}^{\infty} \sum_{m=0}^{\ell} \left(\frac{r_e}{r}\right)^{\ell} P_{\ell m}(\operatorname{Sin}\varphi) \{C_{\ell m} \operatorname{Cos} m\lambda + S_{\ell m} \operatorname{Sin} m\lambda\}\right], \tag{1}$$

where μ is the earth's Gaussian gravity constant (3.98601×10^5 km^3/sec^2), r is the radius from the earth's center of mass to the satellite's, r_e is the mean equatorial radius of the earth (6378.16 km), φ is the satellite's geocentric latitude and λ is its geocentric longitude[7]. The gravity coefficients $C_{\ell m}$ and $S_{\ell m}$ represent longitude dependent harmonic terms ($H_{\ell m}$) when $m \neq 0$. These are the terms which concern us here, and in particular, for the high altitude 24 hour satellites, only the lowest orders (ℓ) of these terms (approximately for $\ell \leq 4$), because of the distance dumping factor $(r_e/r)^{\ell}$ in the potential function of equation (1). The more easily visualized amplitudes $J_{\ell m}$ and phase angles $\lambda_{\ell m}$ of the harmonic terms ($H_{\ell m}$) are related to the $C_{\ell m}$, $S_{\ell m}$ coefficients of these terms by the formulas:

$$J_{\ell m} = [C_{\ell m}^2 + S_{\ell m}^2]^{1/2}$$

$$\lambda_{\ell m} = \frac{1}{m} \operatorname{TAN}^{-1} (S_{\ell m}/C_{\ell m}).$$

With these coefficients, the general disturbing harmonic term $H_{\ell m}$ in Equation (1) can be written as:

$$H_{\ell m} = \left(\frac{r_e}{r} \right)^{\ell} P_{\ell m} (\mathrm{Sin}\,\varphi)\, J_{\ell m} \,\mathrm{Cos}\, m\, (\lambda - \lambda_{\ell m}). \tag{3}$$

It is seen from Equation (3) that the longitude harmonic $H_{\ell m}$ ($m \neq 0$) goes through m undulations in 360° of longitude. Thus we can speak of their wave length as 360°/m and their longitude frequency as m (more accurately, m is the wave number: the number of longitude waves in $H_{\ell m}$ over 360°).

The long term east-west drift of the 24 hour satellite is dominated by a resonance with the H_{22} term of the earth's potential which has the characteristics of pendulum motion[4,8]. In fact all the longitude dependent terms in Equation (1), contribute to this resonance as long as ℓ - m is even. However, due to the distance damping of the anomalous potential, the H_{22} term dominates the drift evolution. The dynamics of this long term pendulum-resonant drift is summarized by the following coupled equations[9], giving the motion of the equator crossing longitudes (λ) and the semimajor axis (a) of the orbit:

$$\ddot{\lambda} = 12\,\pi^2 \sum_{\ell - m\ \mathrm{EVEN}} F_{\ell m} \,\mathrm{Sin}\, m\, (\lambda - \lambda_{\ell m}) \;\frac{\mathrm{rad}}{\mathrm{sideral\ day}^2}, \tag{4}$$

and

$$\dot{a} = -4\pi a_s \sum_{\ell - m\ \mathrm{EVEN}} F_{\ell m} \,\mathrm{Sin}\, m\, (\lambda - \lambda_{\ell m}) \,\frac{\mathrm{a\ units}}{\mathrm{sidereal\ day}}. \tag{5}$$

The relevant coefficients $F_{\ell m}$, to fourth order, $\ell \leq 4$, are given as:

$$F_{22} = \frac{6 J_{22}}{a_s^2} \,[(\mathrm{Cos}\ i + 1)/2]^2$$

$$F_{31} = \frac{-3 J_{31}}{2 a_s^3} \left\{ \frac{(1 + \mathrm{Cos}\ i)}{2} - \frac{5\ \mathrm{Sin}^2\, i\ (1 + 3\ \mathrm{Cos}\ i)}{8} \right\}$$

$$F_{33} = \frac{45 J_{33}}{a_s^3} \left[(\text{Cos } i + 1)/2\right]^3$$

$$F_{42} = \frac{-15 J_{42}}{a_s^4} \left\{ \frac{(1 + \text{Cos } i)^2}{4} - \frac{7 \,\text{Sin}^2 i \,\text{Cos } i \,(1 + \text{Cos } i)}{4} \right\}$$

$$F_{44} = \frac{420 J_{44}}{a_s^4} \left[(\text{Cos } i + 1)/2\right]^4 \qquad (6)$$

The synchronous semimajor axis a_s [in units of earth radii in Equation (6)], is that semimajor axis at which $\dot{\lambda} = 0$. The orbital inclination is i .

Equations (4) and (5) can be combined to eliminate their dependence on the forcing terms and yield an equivalent of Kepler's period law. Thus:

$$\ddot{\lambda}\,(-4\pi a_s / 12\pi^2) = \dot{a}, \text{ or}$$

$$\ddot{\lambda}\,(1/3\pi) + \dot{a}/a_s = 0. \qquad (7)$$

Integrating Equation (7) and evaluating the constant of integration by specifying the synchronous condition, $\dot{\lambda} = 0$ when $a = a_s$, yields:

$$\dot{\lambda} = -3\pi\,(a - a_s)/a_s, \ \frac{\text{rad.}}{\text{sid. day}} \qquad (8)$$

A first integral of Equation (4) can be immediately written down upon the separation of the variables $(\dot{\lambda})^2$ and λ , since $\ddot{\lambda} = d\,(\dot{\lambda})^2/2d\lambda$, yielding:

$$(\dot{\lambda})^2 = C - 24\pi^2 \sum_{\ell - m \text{ EVEN}} (F_{\ell m}/m) \,\text{Cos}\, m\,(\lambda - \lambda_{\ell m}), \ (\text{rad./sid. day})^2, \qquad (9)$$

where C is an arbitrary constant of integration.

Equations (4), (5), (8) and (9) constitute the principal condition equations governing the evolution in longitude and semimajor axis, of the 24 hour satellite due to the earth's anomalous potential. Using position (λ) and velocity or semimajor axis (a) data derived from the tracking of these satellites, we can solve these equations for the relevant longitude gravity harmonics which govern the drift. The semimajor axis data is taken directly from the sets of published mean elements for these satellites (Appendix A). The equator crossing longitudes (λ) are derived from the published sets (Appendix A) of vector (or osculating) elements, by numerical integration for less than one revolution in a realistic earth-moon-sun gravity field.

Where the satellite's drift rate is slow ($\dot{<}$ .15°/day) and the crossing longitudes do not change significantly, the longitude acceleration and semimajor axis drift rate are essentially constant. For these drift arcs a low degree polynomial in the time can be used to determine the acceleration from the crossing or semimajor axis data directly. Where the satellite's drift rate is more rapid it has been found to be most convenient to analyze the data according to the energy integral of the perturbed motion, Equation (9). Consecutive observations of the crossing longitudes from the same or neighboring sets of elements can serve to define the longitude rate over a small longitude range. Alternately, if semimajor axis data is given, Equation (8) defines the drift rate, with the mean synchronous semimajor axis being approximately 6.611 earth radii for both the 33° inclined and equatorial orbit satellites.

For the purposes of this report, all the data in the fast drift arcs were reduced to a single best determined longitude acceleration near the middle of these arcs. This acceleration was determined from Equation (4) using resonant gravity coefficients determined by a least-squares fit of semimajor axis or drift rate data according to Equations (8) and (9). In order to achieve the greatest precision in this acceleration measurement, with the limited data in each arc, only the dominant gravity terms (H_{22} and occasionally H_{33}) were solved for in this preliminary fit. There is some gravity information lost in this preliminary smoothing process for the fast drift arcs. This will be recovered in future analyses of the slow drift (acceleration) data, and the fast drift (drift rate) data combined in a simultaneous solution for all the relevant gravity harmonics.

In Appendix A is found the sets of elements and related tracking data in 13 separate free drift 24 hour satellite arcs. Some of this data, and its reduction to acceleration-points, has already been reported[4], namely data arcs 1, 2, 3, 4, 5, 6, 7, 8-1 and 9-1. A summary of this acceleration-point data reduction (processed by the methods described above for the slow and fast drift arcs) is presented for all the arcs, old and new, in Table 1. Only the old data arc 3 was rejected as too poorly determined to be useful in the gravity solutions. The new drift arcs (10, 11, 12 and 13) of Syncom 3 and Early Bird came about from the following orbit maneuvers:

Arc 10, Syncom 3 (March-May 1965).

The last orbit maneuvers on Syncom 3, performed by NASA, took place in the latter half of March 1965, resulting in a mean motion change from a slow westward to a slow eastward drift at about 172° east longitude. Subsequently this satellite was tracked and operated by DOD (Air Force System Command, Sunnyvale, California). From the last week in March to the end of April there was free drift from 172° to 173 1/2°. An orbit maneuver, only affecting the mean motion, reversed the slow eastward drift to a slow westward drift at the end of April. Free drift followed till the satellite reached about 172° at the end of May 1965. The total period from the end of March till the end of May has been analyzed as a single, slow, free drift arc (10) with a break in the drift rate on 26 April 1965 (Appendix A). An orbit maneuver on Syncom 3, apparently took place in early June 1965 and again on 16 July. Free drift was allowed between 16 July and 5 October 1965, but there are too few observations available during this period to compute a good acceleration.

Arc 11, Syncom 3 (October – March 1965/66)

Orbit maneuvers on Syncom 3 were performed on 5, 19 and 29 October 1965. From 29 October to June 1965/66 Syncom 3 was in a period of slow free drift from 172° to 165-1/2° east longitude. The complete record through March 1966 is analyzed from the data in Appendix A.

Arc 9-2 to 9-5, Early Bird, (July – Nov. 1965)

The Early Bird Arc labeled 9 (April – June 1965) in Reference [4] is here called 9-1. The free drift period for Early Bird between the end of April and the end of 1965 is actually only broken by a major mean motion change maneuver on 2 December 1965. Four newly analyzed portions of free drift Arc 9 (Early Bird) are found in Appendix A, extending from 28° to 38° west longitude.

Arc 12, Early Bird (December – May 1965/66)

After the maneuver on 2 December 1965, the next Early Bird maneuver occurred on 20 September 1966. Five sub-arcs in this new free drift period for Early Bird have been analyzed in Appendix A. They cover the available record to May 1966, and extend from 38° to 28° west longitude.

Arc 13, Syncom 3 (September – January 1966/67)

Orbit maneuvers were performed on Syncom 3 in June and late August 1966. A long, very slow, free drift period ensued from September 1966 through January 1967, carrying the satellite from 161° to 160° east longitude.

In addition to these new free drift arcs, the arc labeled 8 (Syncom 2) in Reference [4], has been extended to cover the continuing slow free drift of Syncom 2 from May 1965 to March 1966 between 65° and 83° east longitude.

The estimates of model bias in Table 1 require some explanation. Initially, the crossing and semimajor axis data are reduced to acceleration points according to the slow or fast drift models discussed previously. Many numerical calculations have shown[4] that sun and moon gravity effects on 24 hour satellites cause long term east-west accelerations of about 0.03×10^{-5} radians/sidereal day^2 (1σ). Calculations also show that radiation pressure without consideration of the earth's shadow, causes a long term acceleration as high as 0.006×10^{-5} rad./sid. day^2 on the Syncom-Early Bird satellites. Taking into account the earth's shadow, I have estimated (from numerically calculated trajectories), the radiation pressure effect to be 0.086×10^{-5} rad./sid. day^2 (1σ). For many of the data arcs, more exact estimates of the gravity biases are available. These biases, due to the sun and moon as well as an incomplete earth model (in the fast drift reductions) were calculated from numerical trajectories closely paralleling the actual trajectories in these arcs. These calculated biases are likely to have errors of 0.005×10^{-5} rad./days^2 (1σ) due to short period effects. The numerical trajectories were calculated by Goddard Space Flight Center's "ITEM" Program (Interplanetary Trajectory by an Encke Method) in the presence of the sun and moon as well as an earth with realistic 2nd and 3rd order longitude gravity effects. For the fast drift arcs reduced to accelerations with only a 2nd order longitude gravity model (including the effects of only $H_{\ell m} = H_{22}$ for $m \neq 0$), the total model biases are estimated to be between 0.040 and 0.045×10^{-5} rad./ sid. day^2 (1σ). For the slow drift arcs, the total model biases are estimated to be 0.035×10^{-5} radians/sid. day^2 (1σ). Where the long term gravity model biases are calculated, the remaining bias, from radiation pressure and short period gravity effects, is estimated to be 0.010×10^{-5} (1σ).

Measured accelerations, due just to the earth's longitude gravity field, are calculated by adding these acceleration bias estimates to the acceleration reduced observations. In Table 1, two sets of measured accelerations are tabulated: one with the calculated major sun-moon bias removed, and one without this adjustment. In both sets, the bias deviations have been added to the measurement deviations. Total 1σ measurement errors are estimated to be the square root of the sums of these deviations.

RESULTS

Table 2 summarizes the gravity results of fitting the acceleration point data in Table 1 to the resonant drift model of equation (4). Of the five gravity terms whose maximum effects should be discernible by this data[4], (H_{22}, H_{31}, H_{33}, H_{42} and H_{44}), only four (H_{22}, H_{31}, H_{33}, H_{44}) had significant effect in reducing the residuals (s) of the experiment. Least squares fits of both the adjusted and unadjusted (unweighted and weighted) data to combinations of these coefficients show a strong reduction in the residuals (over a simple H_{22} fit) only when the terms of H_{33} are included in the model. A comparison of Test 1 with 2, 3, and 4 shows this strong reduction in both the residuals and the standard deviation for the dominant H_{22} coefficients. The validity of the H_{22} solutions in these tests, is also strengthened by the consistency of the coefficients shown in all the tests except perhaps in those for a full field to fourth order (excluding H_{42}). Even in the full field solutions (tests 9 and 10), the divergent values of H_{22} are compensated by a considerably larger standard error in the coefficients which is sufficient to overlap the simpler field solutions. With good data having sufficient longitude coverage, we would expect any of the terms H_{22}, H_{31}, H_{33} and H_{44} to show consistent solutions regardless of the model assumed. Even the small effect of H_{42} may be separable from H_{22}, which has the same longitude frequency, when better data on the moderately inclined Syncom 2 becomes available. As shown in Reference [4], H_{42} has almost no effect on Syncom 2, but a discernible one on the equatorial satellites. The difference would be detectible, resulting in a significant solution for H_{42}, if enough good acceleration data on both Syncom 2 and the equatorial satellites [with errors less than 0.015×10^{-5} rad./sid. day^2 (1σ)] were known.

It is apparent from tests 1 - 10 in Table 2 that the strongest solutions for the harmonics, with this limited record, are achieved with the H_{22}, H_{33} combination tests (2, 3, and 4) even though including H_{31} and H_{44} in the solutions (Tests 9 and 10) result in the lowest residuals. The harmonic coefficients themselves (H_{22} and H_{33}) are best determined in Test 3 on unadjusted but weighted data. The residuals in this test are about 0.013×10^{-5} rad./sid. day^2 greater than in the test with the least residuals (10). But the major coefficients appear better determined in the simpler field test because the solution overadjusts unrealistically for the minor effects in the complex field solutions.

Comparing the tests on weighted unadjusted data (3, 5, 7 and 9) against those on weighted adjusted data (4, 6, 8 and 10), we see apparently the same kind of unrealistic overadjustment for small effects damaging the solution with the more accurate data. The unadjusted data solutions are not heavily constrained towards critical data points. They are generally smoother solutions with somewhat smaller coefficient variance. However, the coefficient variance differences are minor and the adjusted data solutions are more faithful to better data. Therefore I prefer these solutions in all cases where more than H_{22} and H_{33} are being solved for and it is important to be as sensitive as possible to the best measurements. The tests for H_{22} and H_{33} (2, 3, and 4) show little to choose between the use of adjusted, unadjusted, weighted or unweighted data. In both adjusted and unadjusted data tests, there is a noticeable reduction in the residuals when H_{31} is added to the model but at a small sacrifice in the H_{22} and H_{33} coefficient variances (compare tests 3 and 5, and 4 and 6). The smallest residuals of all are achieved with the adjusted data and a four term fit (Test 10). However, the variances in H_{22} appear to be excessive in this test. I believe the longitude survey is still too limited in quality and extent to provide realistic four term estimates.

The lowest residual three term test with reasonable variances appears to be Test 6, and this was finally chosen as the basic solution. This solution is compared point for point with the adjusted measured data, in Table 3 (Column 1 vs. column 2). It is seen in this comparison that all points in the solution are within 3σ of the measured data, 97% of the points are within 2σ and 75% of the points are within 1σ. The same number of points have positive as have negative residuals. These overall statistics are quite favorable. If the residuals were normally distributed, more than 99.7% of them should be within 3σ, 95.5% within 2σ and 68.5% within 1σ. The test 6 solution is a bit better than all the expectations which, of course, are based on an infinite number of data.

The gravity parameters and covariance statistics of the basic solution is also illustrated in Figure 1, which is a calculation, from Equation (4), of the east-west acceleration on a geostationary satellite around the equator. The standard error estimation of this acceleration (the 10σ curve) is particularly revealing. It conforms quite well with the measured data statistics in Table 3. A representative sample of these statistics are displayed as solid vertical lines in Figure 1. The overall 10σ curve of the basic solution clearly reveals those longitudes where data is most needed to strengthen the resonant gravity solution for 24 hour satellites. The overall fit of the basic solution shows a 1σ variation which is always less than 0.1×10^{-5} rad./sid. day^2. Arbitrarily, I use an error of 0.075×10^{-5} rad./day^2 as defining the upper limit of acceptability for the solution. This defines three longitude zones where new data of reasonable quality can be expected to have the greatest effect in strengthening the overall validity of the gravity solution. Positioning a 24 hour satellite between about 12° and 55° east longitude, where no data exists, would probably yield the greatest improvement in geodetic information. Satellites in the zones between about 100° and 157° west longitude, and between approximately 100° and 119° east longitude would also strengthen the 24 hour gravity solution considerably. (These conclusions are also supported in Reference [10].) By a strengthened solution, I mean most of all the reduction in the rather large uncertainty still remaining in the determination of the third order resonant gravity effects. Figure 2 shows the magnitude of this problem. From the error statistics of the basic solution, 1σ probability ellipses (solid curves) have been drawn in the H_{22}, H_{31} and H_{33} quadrants enclosing areas of likely solutions with the limited model as seen by the data (See Appendix B). The ellipses in the H_{22} and H_{31} quadrants are quite extensive, especially the H_{31} ellipse, compared with that defining the variability of the H_{22} effect. Perhaps more important is the large amount of cross correlation in the basic solution between many of the gravity coefficients. This indicates most surely that effects of 2nd and 3rd order are not yet well separated. Once again, this is due undoubtedly to the limited extent of the longitudes surveyed so far by 24 hour satellites.

As stated in the introduction the aim of this investigation is to derive realistic values for the individual gravity terms, as well as good estimates for the east-west accelerations. Therefore it is necessary to consider the likely variance in the basic solution due to the neglect of higher order resonant gravity effects which cannot be well solved for from the limited data available. In fact, solutions 2, 3, and 4 compared to the basic solution may be considered to be an example of such an estimate, since H_{31} is obviously not well determined in the basic solution. As displayed in Figure 2 (x symbol) solution 4 gives estimates of H_{22} and H_{33} outside the basic solution 1σ ellipses for these harmonics. Solutions 7, 8, 9 and 10 with other three and four parameter models also illustrate additional variance possibilities in H_{22}, H_{31} and H_{33}. We can also test for limited-model bias by assuming unmodeled effects here have been well determined by other geodetic satellites and ground surveys. Table 4 lists coefficient values from a number of such recent determinations. All of these except Izsak's 1965 values (which were updated in the SAO 1966 determination) are displayed in Figure 2 for comparison with the 24 hour satellite results. Fixing H_{31}, H_{42} and H_{44} according to the results of Kaula (1966a) as an example, Solution 4 (Table 2) with the limited H_{22}, H_{33} model (adjusted-weighted data) becomes Solution 12). Fixing H_{42} and H_{44} by Kaula's 1966a values, the basic solution (6) becomes Solution 11. It is interesting, and perhaps significant that Solution 11 is little different from the basic solution in spite of the inclusion of higher order effects from an external source. On the other hand Solution 12 shows a rather strong divergance (and increased residuals) from Solution 4. It is seen from Figure 2 that there is quite a large separation of the Solution 6 H_{31} determination from those of recent investigations. We know from the effect on the residuals that H_{31} does have a noticeable influence on the solution. The discrepancy in H_{31} as seen by the 24 hour satellites, while not as great as with still more limited data [compare with the symbols in Figure 2] is still sufficient to suggest there may be more uncertainty in both the H_{22} and H_{33} results than is shown in the statistics of the basic solution. This conclusion is supported by the previous comparison between the simple two parameter solutions (2, 3, and 4) and the basic three parameter solution (6).

Summarizing, the dashed rectangles in Figure 2 are realistic estimates of the likely absolute bounds on H_{22}, H_{31} and H_{33} as assessed by the 24 hour satellites so far (see Appendix B). They take into consideration the model simplifications forced on the solution due to the limited data available through 1966. The total variability in the coefficients from the basic solution over all the tests in Table 3, was the main criteria in setting these realistic bounds. Some discretion was exercised, however, in crediting the extremes of the variability in H_{22} from the simplest solution, Test 1, and in H_{22} and H_{31} from the most complex andprobably overadjusted solutions, Tests 9 and 10.

An interesting aspect of the results of the statistics of the "basic solution" is that the 1σ ellipse does point in the direction of the most recent geodetic determinations (Figure 2). In fact, the 2σ H_{31} ellipse actually overtakes these values, but without enclosing them by a small margin. However, an examination of the correlation coefficients of this solution is not as encouraging as this simple observation suggests. It is true that the H_{22}, C_{33} coefficients are strongly and positively correlated. Thus movement in the H_{22} ellipse towards the predominant recent determinations is also correlated to movement in the H_{33} ellipse towards these same solutions. However, the H_{31} correlation coefficients H_{22} and C_{33} are strongly negative so that the movement towards the predominant recent solutions in the H_{22} and H_{33} ellipses is strongly correlated to movement away from these solutions in the H_{31} ellipse. Evidently, the direction of these ellipses suggest better agreement to recent results than is actually indicated by the data.

A further comparison of three of these recent determinations, directly with the adjusted 24 hour satellite measurements, is displayed in Table 3. From this comparison, it is apparent that the solution which best represents the 24 hour observations is that of Kaula (1966a). The Kaula 1966b solution ($\triangle$ symbols in Figure 2) would, evidently, compare best of all with the 24 hour data, but that is because this solution incorporates in it a fair amount of this data. In fact the Kaula (1966a) solution, indirectly is also weighted towards the 24 hour data; but to a smaller degree than that of Kaula (1966b). Considering independent solutions along, SAO (1966) appears to be a somewhat superior solution than Anderle (1965) on the basis of the 24 hour satellite data. Comparing the two Doppler-Satellite solutions from Figure 2, the Anderle one would probably prove somewhat better overall, than that of Guier and Newton, because of its closer H_{22} agreement with the 24 hour satellite solution. But clearly, all of these recent solutions have failed to predict even reasonably well, the accurate accelerations measured in the Early Bird arcs.

A graphical display of the unadjusted and adjusted and predicted accelerations in the Early Bird and Syncom 3 arcs as well as in the last Syncom 2 drift period, is shown in Figure 3.

As incidental, but important statistics from the basic solution, the four equilibrium points (zero acceleration) for the geostationary satellite are located at (See Figure 1):

$$\lambda_1 = 75.9 \pm 0.6^\circ \text{ (Stable Equilibrium)}$$

$$\lambda_2 = 161.9 \pm 0.3^\circ \text{ (Unstable Equilibrium)}$$

$$\lambda_3 = -106.7 \pm 0.9^\circ \text{ (Stable Equilibrium)}$$

$$\lambda_4 = -11.9 \pm 0.5^\circ \text{ (Unstable Equilibrium)}.$$

All of these values except for λ_3 are within the 1σ estimates given in Reference [4] from more limited data. The bounds on λ_3 given here overlap those determined in the earlier study.

The maximum east-west acceleration on the geostationary satellite, due to the earth, occurs at 119° east with a magnitude of $-3.18 \pm 0.08 \times 10^{-5}$ rad./sid. day^2 = $-1.83 \pm 0.5 \times 10^{-3}$ deg./solar day^2. This is identical to the result of the earlier study[4], so that, to correct continuously for this east-west acceleration would require (as calculated previously) conservatively, a velocity increment of:

$$\Delta V = 6.38 \text{ ft./sec./yr.}$$

Finally, as a check on these results, we can compare the coefficients seen in this new solution, with those seen in the earlier study[4]. The new solution (Table 2 and Figure 2) is, except for the ill determined H_{31} coefficients, within the 1σ bounds found in the earlier study. The coefficients absolute bounds in this new solution are, however, greater than those in the old study, in spite of the fact that more and better data has been used here. This conservatism is due, principally, to the method of evaluating the model bias effects. Here these effects are estimated by direct comparison of many parameter tests on the actual acceleration record, with and without use of external gravity information. In the older study, the likely model bias was evaluated only indirectly from simulated data which was of a much higher quality than the actual acceleration record.

As a result, it appears from this study that only H_{22} (rather than both H_{22} and H_{33}) is significantly better determined from the available 24 hour satellite record, than in any of the other recent geodetic reductions.

CONCLUSIONS

1. As in the previous study of 2 years of the 24 hour satellite record[4], I conclude that virtually all of the east-west geographic acceleration of the 24 hour satellites can be accounted for by the second and third order sectorial harmonics of the earth's gravitational field which resonate with them.

2. With due adjustment for the small long term effects of the sun and moon's gravity and radiation pressure, and considering the neglect of likely higher order resonant earth gravity, these dominant sectorial harmonics are estimated to be:

$$10^6 J_{22} = 1.80 \pm 0.04,$$

which corresponds to a difference in major and minor radii of 68.8 ± 1.8 meters in the earth's elliptical equator; and

$$\lambda_{22} = -15.3 \pm 0.6^\circ,$$

which is the longitude location of the major axis of the elliptical equator, and

$$10^6 J_{33} = 0.16^{+0.05}_{-0.03},$$

$$\lambda_{33} = 26.4^{+6.6^\circ}_{-8.3^\circ}.$$

3. The sectorial harmonics above, within their ranges, are believed to be absolute or true measures of those individual components of the earth's field.

4. A third resonant earth harmonic, H_{31}, was evident but poorly discriminated from the limited acceleration record. The data shows the absolute bounds on this harmonic to be:

$$10^6 J_{31} = 1.5^{+2.6}_{-1.2}, \text{ and}$$

$$\lambda_{31} = -79^{+73^\circ}_{-88^\circ}.$$

5. The 3-1/2 year record of 24 hour satellite accelerations shows that the geostationary satellite can be in uncontrolled long term east-west equilibrium at only the following four longitude locations:

$$\lambda_1 = 75.9 \pm .6^\circ \text{ (Stable Equilibrium)}$$
$$\lambda_2 = 161.9 \pm .3^\circ \text{ (Unstable Equilibrium)}$$
$$\lambda_3 = -106.7 \pm .9^\circ \text{ (Stable Equilibrium)}$$
$$\lambda_4 = -11.9 \pm .5^\circ \text{ (Unstable Equilibrium).}$$

6. The maximum long term longitude acceleration on the geostationary satellite is, as reported previously:

$$\ddot{\lambda} = -1.88 \times 10^{-3} \text{ deg./day}^2,$$

occurring at about 119° east of Greenwich, and requiring a velocity increment of 6.38 ft/sec/year to counteract continuously.

7. The H_{22} term, measured from this 3-1/2 year data record, is probably the most accurate known at this time. However, the accurate measurement of H_{31}, H_{33} and higher order effects must wait on receipt of new high quality tracking data, especially from longitudes not covered by the operating 24 hour satellites studied here.

REFERENCES

1. Wagner, C. A., "Longitude Variations in the Earth's Gravity Field as Sensed by the Drift of Three Synchronous Satellites," Journal of Geophys. Res., 71, No. 6, 1703-1712, 1966.

2. Allan, R. R., "Even Tesseral Harmonics in the Geopotential Derived From Syncom 2," Proceedings of the Second International Symposium on the Use of Artificial Satellites for Geodesy; Athens, Greece, April 1965.

3. Wagner, C. A., "Determination of the Ellipticity of the Earth's Equator From Observations on the Drift of the Syncom 2 Satellite," NASA TN-D-2759, 1965.

4. Wagner, C. A., "The Earth's Longitude Gravity Field as Sensed by the Drift of Three Synchronous Satellites," NASA TN-D-3557, 1966.

5. King-Hele, D. G. and Cook, G. E., "The Even Zonal Harmonics of the Earth's Gravitational Potential," Geophys. Journal 10, 17 (1965).

6. King-Hele, D. G., et al., "The Odd Zonal Harmonics in the Earth's Gravitational Potential," Planet. Space Sci. 13, 1213 (1965).

7. Kaula, W. M., "Theory of Satellite Geodesy," Blaisdell Press, Waltham, Mass. (1966).

8. Allan, R. R., "On the Motion of Nearly Synchronous Satellites," Proc. Roy. Soc. A288, 60 (1965).

9. Wagner, C. A., "The Use of Resonant Librating Orbits in Satellite Geodesy," NASA TN-D-4081, 1967.

10. Allan, R. R. and Piggott, B. A. M., "Longitude Dependence of the Geopotential Deduced from Synchronous Satellites," Royal Aircraft Establishment Report (October 1966).

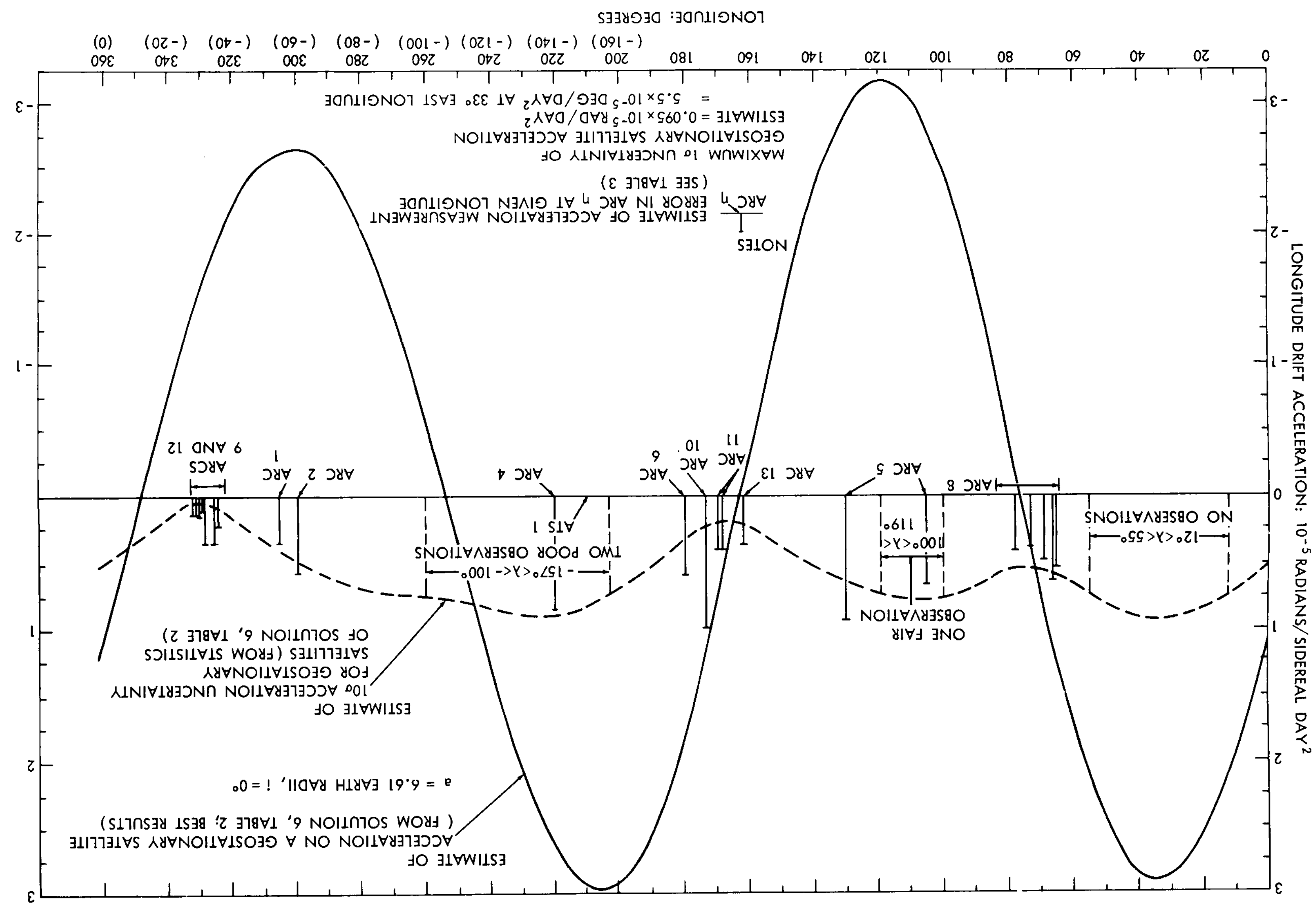

Figure 1. Drift Acceleration and Estimate of Acceleration Uncertainties on 24 Hour Satellites.

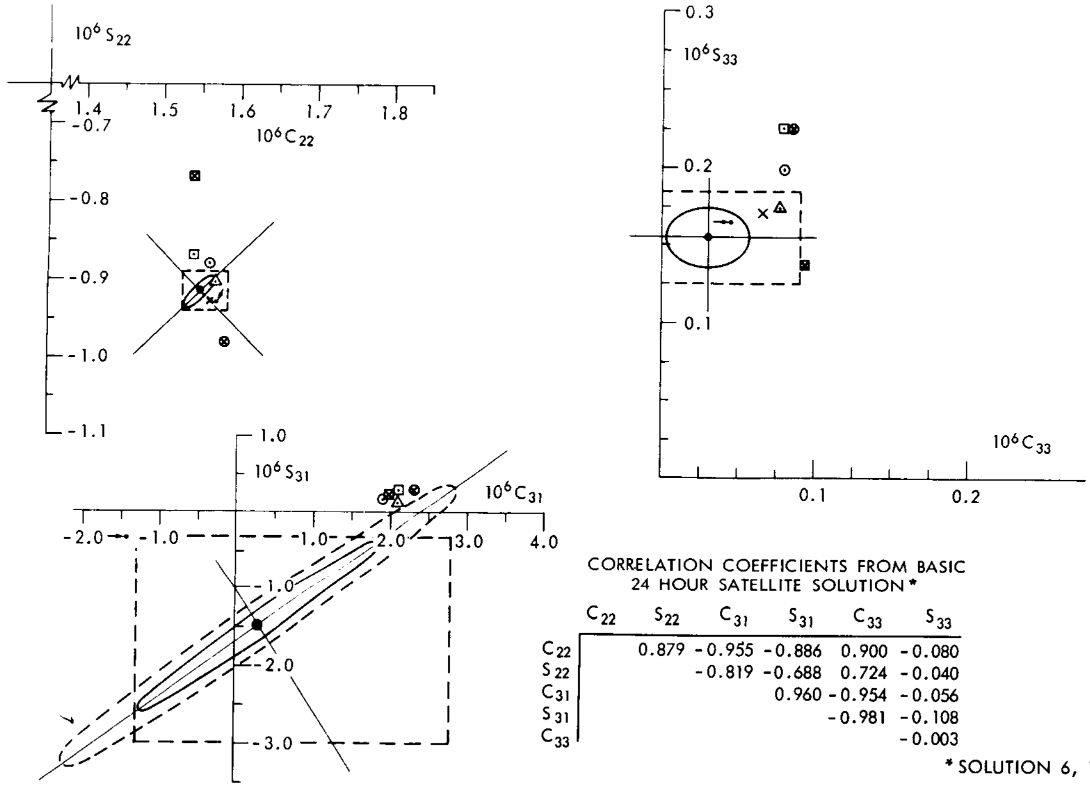

CORRELATION COEFFICIENTS FROM BASIC 24 HOUR SATELLITE SOLUTION*

	C_{22}	S_{22}	C_{31}	S_{31}	C_{33}	S_{33}
C_{22}		0.879	-0.955	-0.886	0.900	-0.080
S_{22}			-0.819	-0.688	0.724	-0.040
C_{31}				0.960	-0.954	-0.056
S_{31}					-0.981	-0.108
C_{33}						-0.003

*SOLUTION 6, TABLE 2

NOTES:

- BASIC 24 HOUR SATELLITE SOLUTION WITH 1σ (INNER) AND 2σ (OUTER) PROBABILITY ELLIPSES
- ABSOLUTE BOUNDS ON HARMONICS AS ESTIMATED BY 24 HOUR SATELLITES AND OTHER DATA
- ⊙ KAULA (1966a) SOLUTION (SEE TABLE 4)
- △ KAULA (1966b) "
- ⊡ SAO (1966) "
- ○ ANDERLE (1965) "
- □ GUIER AND NEWTON (1965) "
- WAGNER (1966) "
- × H_{22} AND H_{33} SOLUTION 4 FROM 24 HOUR SATELLITE DATA (SEE TABLE 2)

Figure 2. Longitude Gravity Harmonics Affecting 24 Hour Satellites, From Recent Investigations.

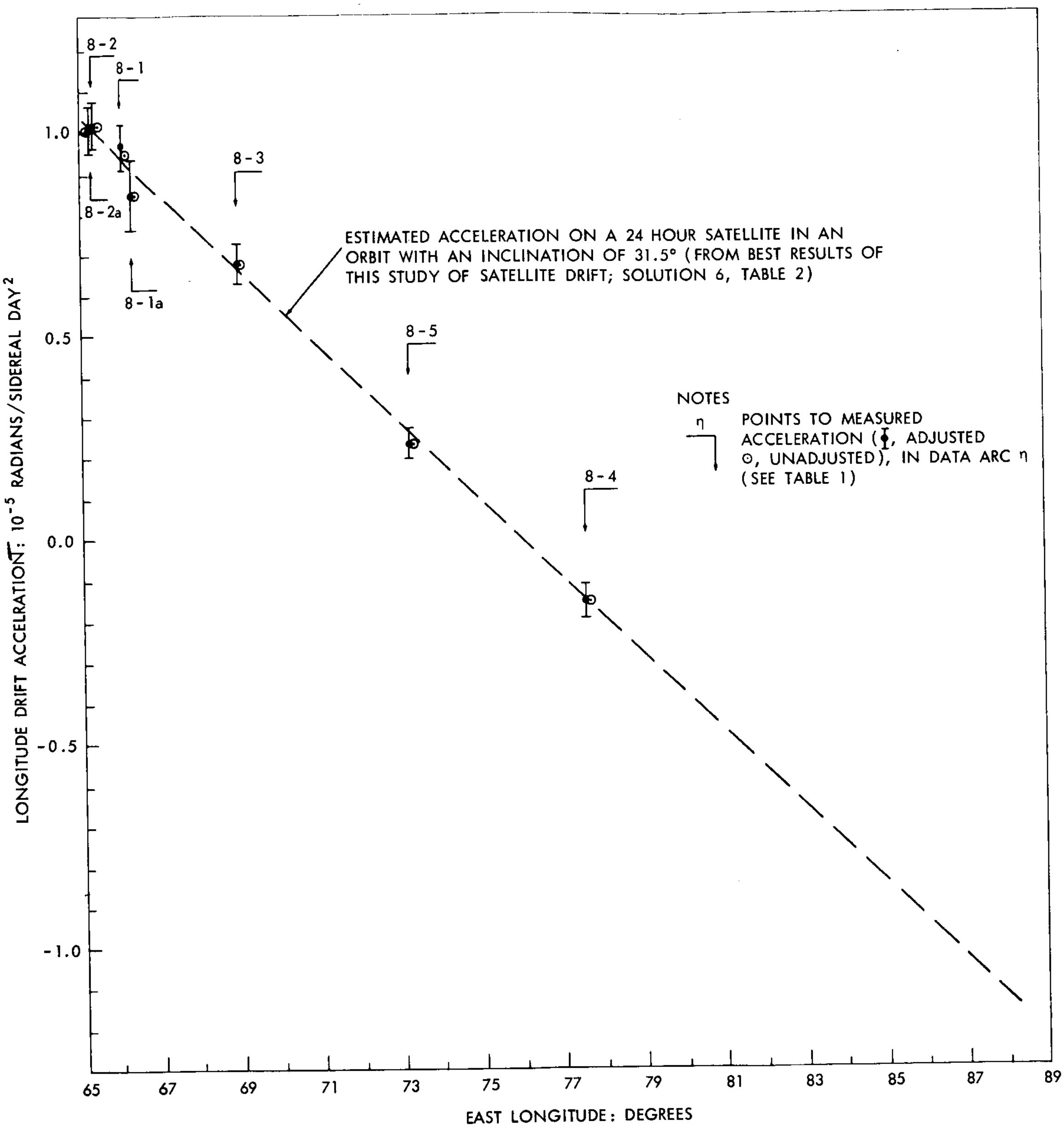

Figure 3A. Drift Acceleration in Syncom 2 Arc 8.

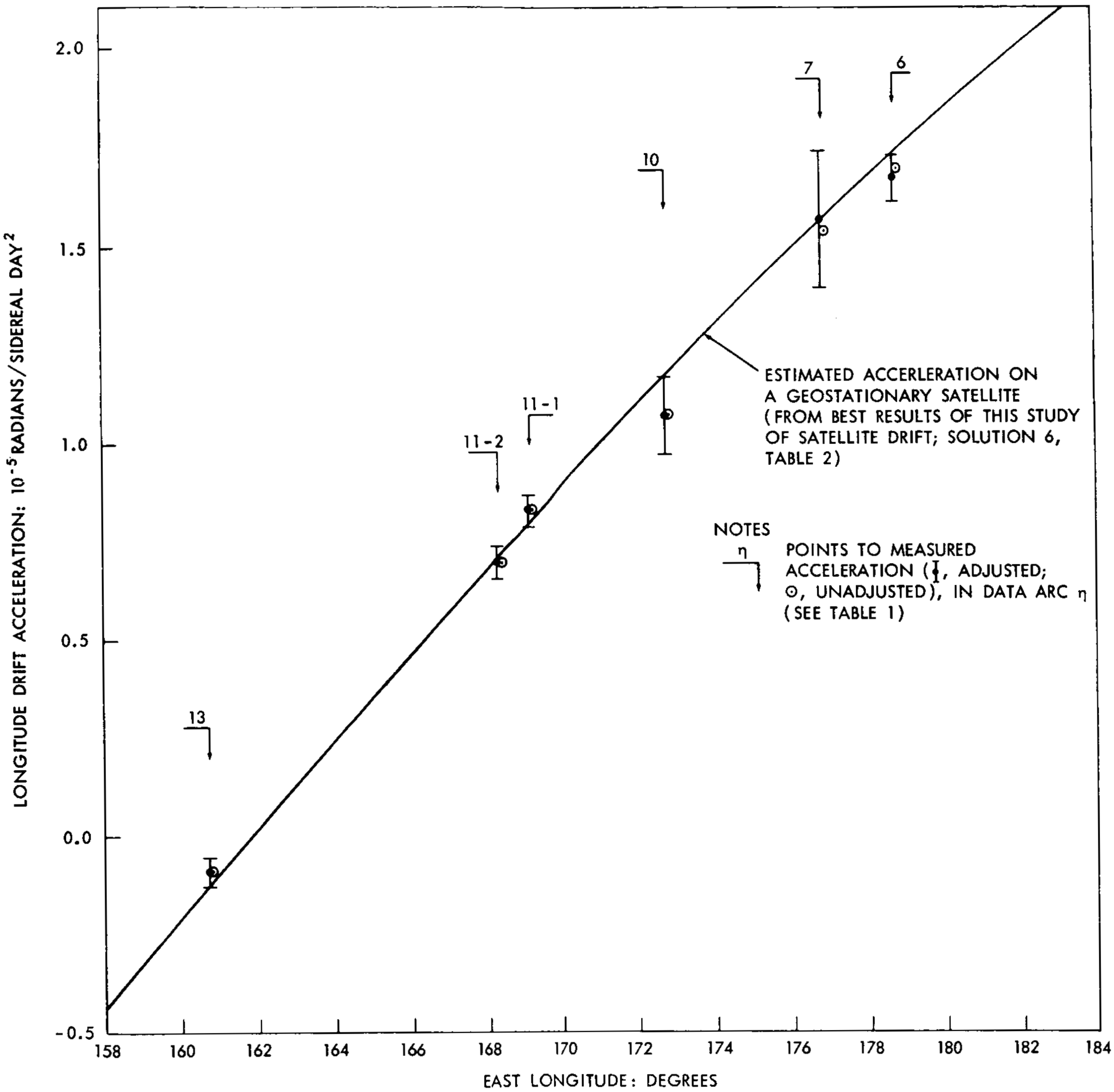

Figure 3B. Drift Acceleration in Syncom 3 Arcs 6, 7, 10, 11 and 13.

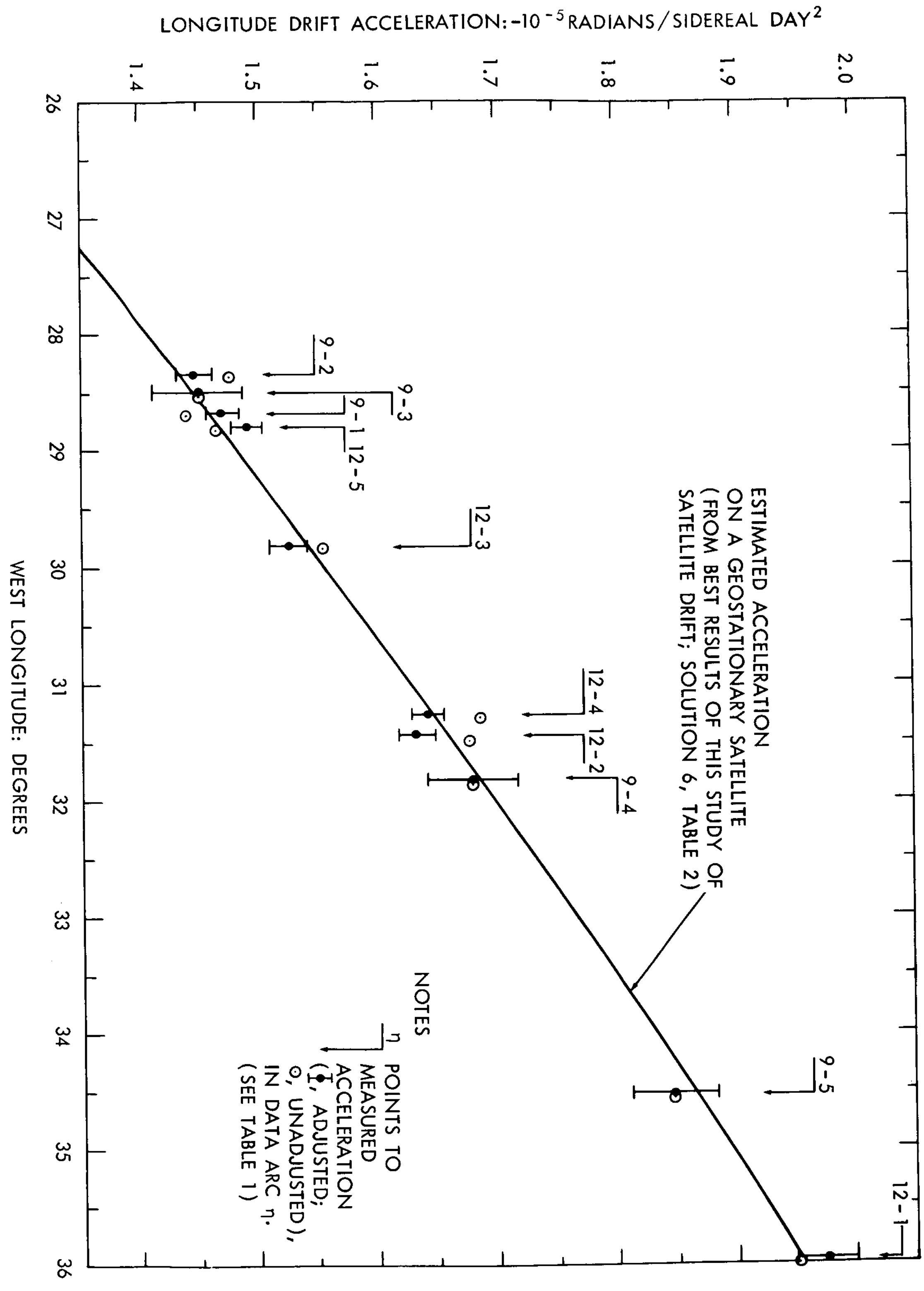

Figure 3C. Drift Acceleration in Early Bird Arcs 9 and 12.

Table 1

Data From 13 Free Drift Arcs of Three 24 Hour Satellites

SATELLITE	① ARC	② LONGITUDE (λ): DEGREES	SEMIMAJOR AXIS (a): EARTH RADII	INCLINATION (i): DEGREES	③ MEASURED DRIFT ACCELERATION ($\ddot{\lambda}$): 10^{-5} RADIANS PER SIDEREAL DAY^2	④ $\sigma(\ddot{\lambda})$, MEASURED: 10^{-5} RADIANS PER SIDEREAL DAY^2	⑤ $\sigma(\ddot{\lambda})$ BIAS, ESTIMATED: 10^{-5} RAD/DAY^2	⑥ $\ddot{\lambda}$ BIAS, CALCULATED: 10^{-5} RAD/DAY^2	⑦ $\ddot{\lambda}$, MEASURED ACCELERATION, UNADJUSTED FOR CALCULATED BIAS: 10^{-5} R/D^2	⑧ $\ddot{\lambda}$, MEASURED ACCELERATION, ADJUSTED FOR CALCULATED BIAS: 10^{-5} R/D^2
SYNCOM 2	1	-55.22	6.6111	33.02	-2.253	0.033	0.035	+0.015 ±0.010	-2.253 ±0.048	-2.238 ±0.035
SYNCOM 2	1a	-55.235	6.611	33.02	2.255	0.078	0.035		-2.255 ±0.086	-2.255 ±0.086
SYNCOM 2	2	-60.94	6.6116	32.825	-2.291	0.057	0.035	-0.029 ±0.010	-2.291 ±0.067	-2.320 +0.058
SYNCOM 2	2a	-61.00	6.612	32.83	-2.288	0.117	0.035		-2.288 ±0.122	-2.288 +0.122
SYNCOM 2	4	-140.00	6.6204	32.58	2.138	0.084	0.040	+0.015 ±0.010	2.138 ±0.093	2.153 ±0.085
SYNCOM 2	4a	-140.00	6.620	32.58	2.366	0.155	0.040		2.366 ±0.160	2.366 ±0.160
SYNCOM 2	5-1	161.00	6.6165	32.40	-0.199	0.066	0.040	+0.005 ±0.010	-0.199 ±0.077	-0.194 ±0.067
SYNCOM 2	5a	130.00	6.617	32.3	-2.550	0.082	0.045		-2.550 ±0.093	-2.550 ±0.093
SYNCOM 2	5-2	104.50	6.6176	32.15	-2.278	0.066	0.040	-0.041 ±0.010	-2.278 ±0.077	-2.319 ±0.067
SYNCOM 3	6	178.71	6.6115	0.11	1.707	0.059	0.035	-0.024 ±0.010	1.707 ±0.069	1.683 ±0.060
SYNCOM 3	7	176.80	6.6123	0.27	1.550	0.175	0.035	+0.027 ±0.010	1.550 ±0.178	1.577 ±0.175
SYNCOM 2	8-1	66.115	6.6112	31.89	0.950	0.062	0.035	+0.018 ±0.010	0.950 ±0.071	0.968 ±0.063
SYNCOM 2	8-1a	66.39	6.61125	31.89	0.845	0.078	0.035		0.845 ±0.086	0.845 ±0.086
SYNCOM 2	8-2	65.31	6.61095	31.79	1.017	0.040	0.035		1.017 ±0.053	1.017 ±0.053
SYNCOM 2	8-2a	65.30	6.6109	31.78	1.000	0.040	0.035		1.000 ±0.053	1.000 ±0.053
SYNCOM 2	8-3	69.00	6.61	31.4	0.676	0.032	0.035		0.676 ±0.047	0.676 ±0.047
SYNCOM 2	8-4	77.60	6.61	31.4	-0.152	0.021	0.035		-0.152 ±0.041	-0.152 ±0.041
SYNCOM 2	8-5	73.25	6.61	31.4	0.235	0.015	0.035		0.235 ±0.038	0.235 ±0.038
EARLY BIRD	9-1	-28.70	6.6105	0.20	-1.441	0.010	0.035	-0.031 ±0.010	-1.441 ±0.036	-1.472 ±0.014
EARLY BIRD	9-2	-28.37	6.6112	0.43	-1.478	0.010	0.035	+0.030 ±0.010	-1.478 ±0.036	-1.448 ±0.014
EARLY BIRD	9-3	-28.54	6.6112	0.43	-1.453	0.016	0.035		-1.453 ±0.038	-1.453 ±0.038
EARLY BIRD	9-4	-31.86	6.61185	0.55	-1.682	0.014	0.035		-1.682 ±0.038	-1.682 ±0.038
EARLY BIRD	9-5	-34.57	6.6123	0.64	-1.849	0.008	0.035		-1.849 ±0.036	-1.849 ±0.036
SYNCOM 3	10	172.75	6.611	0.00	1.072	0.093	0.035		1.072 ±0.099	1.072 ±0.099
SYNCOM 3	10a*	172.75	6.611	0.00	0.907	0.345	0.035		0.907 ±0.345	0.907 ±0.345
SYNCOM 3	11-1	169.10	6.61	0.53	0.831	0.018	0.035		0.831 ±0.039	0.831 ±0.039
SYNCOM 3	11-2	168.29	6.61	0.53	0.699	0.020	0.035		0.699 ±0.040	0.699 ±0.040
EARLY BIRD	12-1	-35.98	6.6094	0.74	-1.954	0.021	0.035	-0.022 ±0.010	-1.954 ±0.041	-1.976 ±0.023
EARLY BIRD	12-2	-31.46	6.6101	0.85	-1.678	0.010	0.035	+0.045 ±0.010	-1.678 ±0.036	-1.633 ±0.014
EARLY BIRD	12-3	-29.83	6.6101	0.85	-1.556	0.011	0.035	+0.029 ±0.010	-1.556 ±0.037	-1.527 ±0.015
EARLY BIRD	12-4	-31.29	6.6103	0.90	-1.688	0.007	0.035	+0.044 ±0.010	-1.688 ±0.036	-1.644 ±0.012
EARLY BIRD	12-5	-28.83	6.6103	0.90	-1.467	0.006	0.035	-0.027 ±0.010	-1.467 ±0.036	-1.494 ±0.012
SYNCOM 3	13	160.74	6.61	1.3	-0.090	0.010	0.035		-0.090 ±0.036	-0.090 ±0.036

NOTES ① DA.A ARCS 1, 2, 4, 5-1, 5-2, 6, 7, 8-1, AND 9-1 ARE IDENTICAL TO ARCS 1, 2, 4, 5A, 5-18, 6, 7, 8 AND 9 OF REFERENCE [4], TABLE 10. ARCS 1a, 2a, 4a, ETC. ARE ANALYZED FROM SEMIMAJOR AXIS DATA. SEE APPENDIX A FOR THE DATA USED IN ALL THE NEW ARCS.

② THESE ARE THE LONGITUDES NEAR THE MID POINTS OF THE DRIFT ARCS, WHERE THE ACCELERATION IS BEST DETERMINED BY THE DATA (SEE REFERENCE [4] AND APPENDIX A FOR THE LONGITUDE SPAN COVERED IN EACH DATA ARC, AND TABLE 3 FOR THE TIME SPAN IN EACH ARC).

③ THIS IS THE ACCELERATION AS REDUCED FROM THE CROSSING OR SEMIMAJOR DATA BY A SIMPLE LOW ORDER TIME POLYNOMIAL OR ENERGY (DRIFT RATE) INTEGRAL MODEL, AS DESCRIBED IN THE TEXT.

④ THIS IS THE ESTIMATION OF THE MINIMUM STANDARD DEVIATION OF THE ACCELERATION, MEASURED AS DESCRIBED ABOVE AND IN THE TEXT.

⑤ THIS BIAS DEVIATION ESTIMATE IS BASED ON AN ESTIMATE OF $\pm 0.032 \times 10^{-5}$ RAD/DAY^2 FOR SUN-MOON-EARTH MODEL BIAS AND $\pm 0.008 \times 10^{-5}$ R/D^2 FOR RADIATION PRESSURE, FOR THE SLOW DRIFT ARCS, AND AN INCREASE IN THE SUN-MOON-EARTH MODEL BIAS TO $\pm(0.040 \rightarrow 0.045) \times 10^{-5}$ RAD/DAY^2 FOR THE FAST DRIFT ARCS.

⑥ THIS IS THE SUN-MOON-EARTH MODEL BIAS CALCULATED FROM NUMERICALLY GENERATED TRAJECTORIES CLOSELY PARALLELING THE ACTUAL TRAJECTORIES (SEE REFERENCE [4]). THE UNCERTAINTY OF 0.01×10^{-5} RAD/DAY^2 IS DUE TO UNCERTAINTY IN THIS CALCULATION PLUS LIKELY RADIATION PRESSURE BIAS.

⑦ COLUMN ③ DATA WITH DEVIATIONS TAKEN AS THE SQUARE ROOT OF THE SUMS OF THE SQUARES OF THE DEVIATIONS IN COLUMNS ④ AND ⑤.

⑧ COLUMNS ③ + ⑥ DATA WITH DEVIATIONS TAKEN AS THE SQUARE ROOT OF THE SUMS OF THE SQUARES OF THE DEVIATIONS IN COLUMNS ④ AND ⑥.

*. OMITTED FROM THE GRAVITY ANALYSIS; ACCELERATION TOO POORLY DETERMINED.

Table 2

Solutions (Tests) for Gravity Coefficients From 24 Hour Satellite Data

SOLUTION (TEST #)	DATA* (32 PTS)	$10^7 S$** (RAD/DAY^2)	$10^6 C_{22}$	$10^6 S_{22}$	$10^6 C_{31}$	$10^6 S_{31}$	$10^6 C_{33}$	$10^6 S_{33}$	$10^8 C_{44}$	$10^8 S_{44}$
1	UNADJUSTED, UNWEIGHTED	19.8	1.590 ±0.04	-0.970 ±0.04						
2	UNADJUSTED, UNWEIGHTED	5.54	1.578 ±0.011	-0.936 ±0.012			0.051 ±0.009	0.155 ±0.009		
3	UNADJUSTED, WEIGHTED	3.57	1.562 ±0.011	-0.932 ±0.011			0.066 ±0.006	0.168 ±0.007		
4	ADJUSTED, WEIGHTED	2.61	1.558 ±0.012	-0.928 ±0.012			0.064 ±0.007	0.171 ±0.008		
5	UNADJUSTED, WEIGHTED	3.08	1.543 ±0.011	-0.920 ±0.012	-0.57 ±0.83	-1.36 ±0.58	0.027 ±0.013	0.148 ±0.008		
6	ADJUSTED, WEIGHTED	2.49	1.547 ±0.015	-0.913 ±0.014	0.28 ±1.00	-1.47 ±0.74	0.029 ±0.017	0.155 ±0.011		
7	UNADJUSTED, WEIGHTED	3.55	1.551 ±0.013	-0.921 ±0.014			0.064 ±0.010	0.160 ±0.010	-0.29 ±0.67	-1.28 ±0.90
8	ADJUSTED, WEIGHTED	2.71	1.559 ±0.016	-0.927 ±0.018			0.066 ±0.012	0.170 ±0.011	-0.15 ±0.83	0.18 ±1.08
9	UNADJUSTED, WEIGHTED	3.12	1.546 ±0.012	-0.88 ±0.05	1.8 ±3.3	-2.6 ±1.3	0.036 ±0.021	0.133 ±0.018	-1.8 ±2.1	0.23 ±1.4
10	ADJUSTED, WEIGHTED	2.25	1.551 ±0.014	-0.86 ±0.06	3.4 ±3.5	-3.5 ±1.4	0.039 ±0.024	0.127 ±0.021	-3.1 ±2.3	1.1 ±1.7
11	ADJUSTED, WEIGHTED	2.43	1.546 ±0.015	-0.916 ±0.013	0.06 ±0.98	-1.64 ±0.72	0.025 ±0.017	0.154 ±0.011	K66a*** (ALSO H_{42})	
12	ADJUSTED, WEIGHTED	3.15	1.585 ±0.015	-0.931 ±0.014	K66a***		0.087 ±0.008	0.184 ±0.010	K66a*** (ALSO H_{42})	

NOTES
- * SEE TABLE 1 FOR THE SET OF UNADJUSTED AND ADJUSTED DATA USED. WEIGHTS WERE ASSIGNED IN INVERSE PROPORTION TO THE SQUARE OF THE ESTIMATED STANDARD ERROR OF THE MEASURED ACCELERATIONS.
- ** S = ESTIMATE OF STANDARD ERROR (RMS RESIDUAL) FOR GRAVITY SOLUTION OVER ALL THE DATA.
- *** COEFFICIENTS FIXED FROM DETERMINATION OF KAULA (1966 a), SEE TABLE 4.

BEST RESULTS (FROM SOLUTION 6 WITH BOUNDS INCREASED DUE TO LIKELY MODEL ERRORS):

$$10^6 C_{22} = 1.550 \;{}^{+0.035}_{-0.025}, \quad 10^6 S_{22} = -0.915 \;\pm 0.025$$

$$10^6 C_{31} = 0.3 \;{}^{+2.5}_{-1.6}, \quad 10^6 S_{31} = -1.5 \;{}^{+1.2}_{-1.5}$$

$$10^6 C_{33} = 0.03 \;{}^{+0.06}_{-0.03}, \quad 10^6 S_{33} = 0.155 \;\pm 0.030$$

$$10^6 J_{22} = 1.80 \;\pm 0.04, \quad \lambda_{22} = -15.3 \;\pm 0.6^\circ$$

$$10^6 J_{31} = 1.5 \;{}^{+2.6}_{-1.2}, \quad \lambda_{31} = -79 \;{}^{+73^\circ}_{-88^\circ}$$

$$10^6 J_{33} = 0.16 \;{}^{+0.05}_{-0.03}, \quad \lambda_{33} = 26.4 \;{}^{+6.6^\circ}_{-8.3^\circ}$$

Table 3

Measured and Predicted Accelerations on 24 Hour Satellites

				①	②	③	④	⑤
ARC	SATELLITE	LONGITUDE* (DEGREES)	DRIFT TIME	MEASURED** DRIFT ACCELERATION (10^{-5} RADIANS/SID. DAY^2)	PREDICTED DRIFT ACCELERATION (10^{-5} RAD/SID. DAY^2)			
					WAGNER (1967b) (COEFFICIENTS OF TEST 6, TABLE 2)	KAULA (1966a)	SAO (1966)	ANDERLE (1965)
1	SYNCOM 2	-55.22	AUG – DEC '63	-2.238 ±0.035	-2.234	$-2.146^{2\sigma}$	$-2.079^{4\sigma}$	-2.185
1a	SYNCOM 2	-55.24	AUG – DEC '63	-2.255 ±0.086	-2.234	-2.146	$-2.079^{2\sigma}$	-2.185
2	SYNCOM 2	-60.94	DEC – MAR '63 – '64	-2.320 ±0.058	-2.254	$-2.139^{3\sigma}$	$-2.069^{4\sigma}$	$-2.200^{2\sigma}$
2a	SYNCOM 2	-61.00	DEC – MAR '63 – '64	-2.288 ±0.122	-2.254	-2.138	-2.068	-2.199
4	SYNCOM 2	-140.00	APR – JULY '64	2.153 ±0.085	2.189	2.114	2.066	2.140
4a	SYNCOM 2	-140.00	APR – JULY '64	2.366 ±0.159	2.189	2.114	2.066	2.140
5-1	SYNCOM 2	161.00	JULY – FEB '64 – '65	-0.194 ±0.067	-0.141	-0.133	-0.110	$-0.004^{2\sigma}$
5a	SYNCOM 2	130.00	JULY – FEB '64 – '65	-2.550 ±0.093	-2.484	-2.541	-2.557	-2.640
5-2	SYNCOM 2	104.50	JULY – FEB '64 – '65	-2.319 ±0.067	-2.326	-2.433	-2.438	$-2.623^{4\sigma}$
6	SYNCOM 3	178.71	OCT – JAN '64 – '65	1.683 ±0.060	1.749	1.668	1.705	$1.881^{3\sigma}$
7	SYNCOM 3	176.80	JAN – MAR '65	1.577 ±0.177	1.575	1.499	1.536	1.711
8-1	SYNCOM 2	66.12	FEB – JUNE '65	0.968 ±0.063	0.924	0.993	1.021	0.968
8-1a	SYNCOM 2	66.39	FEB – JUNE '65	0.845 ±0.086	0.900	0.967	0.995	0.940
8-2	SYNCOM 2	65.31	FEB – JUNE '65	1.017 ±0.053	0.996	1.069	1.096	1.048
8-2a	SYNCOM 2	65.30	FEB – JUNE '65	1.000 ±0.053	0.997	1.070	1.097	1.049
10	SYNCOM 3	172.75	MAR – MAY '65	1.072 ±0.099	1.181	1.114	1.151	$1.319^{2\sigma}$
8-3	SYNCOM 2	69.00	JULY – MAR '65 – '66	0.676 ±0.047	0.666	0.718	0.747	0.676
8-4	SYNCOM 2	77.60	JULY – MAR '65 – '66	-0.152 ±0.041	-0.160	-0.161	-0.133	$-0.252^{2\sigma}$
8-5	SYNCOM 2	73.25	JULY – MAR '65 – '66	0.235 ±0.038	0.263	0.289	$0.318^{2\sigma}$	0.223
11-1	SYNCOM 3	169.10	NOV – MAY '65 – '66	0.831 ±0.039	0.801	$0.740^{2\sigma}$	0.775	$0.933^{2\sigma}$
11-2	SYNCOM 3	168.29	NOV – MAY '65 – '66	0.699 ±0.040	0.713	0.654	0.688	$0.843^{3\sigma}$
13	SYNCOM 3	160.74	SEPT – JAN '66 – '67	-0.090 ±0.036	-0.127	$-0.181^{2\sigma}$	-0.157	-0.034
9-1	EARLY BIRD	-28.70	APR – JUNE '65	-1.472 ±0.014	-1.463	-1.446	$-1.424^{3\sigma}$	$-1.361^{7\sigma}$
9-2	EARLY BIRD	-28.37	JUNE – AUG '65	-1.448 ±0.014	-1.437	-1.423	$-1.402^{3\sigma}$	$-1.337^{7\sigma}$
9-3	EARLY BIRD	-28.54	JUNE – AUG '65	-1.453 ±0.038	-1.450	-1.435	-1.413	$-1.349^{2\sigma}$
9-4	EARLY BIRD	-31.86	SEPT – OCT '65	-1.682 ±0.038	-1.690	-1.652	-1.618	$-1.577^{2\sigma}$
9-5	EARLY BIRD	-34.57	OCT – NOV '65	-1.849 ±0.036	-1.869	-1.811	$-1.769^{2\sigma}$	$-1.746^{3\sigma}$
12-1	EARLY BIRD	-35.98	DEC – JAN '65 – '66	-1.976 ±0.023	-1.958	$-1.889^{3\sigma}$	$-1.842^{5\sigma}$	$-1.829^{6\sigma}$
12-2	EARLY BIRD	-31.46	JAN – MAR '66	-1.633 ±0.014	$-1.663^{2\sigma}$	-1.628	$-1.596^{2\sigma}$	$-1.551^{8\sigma}$
12-3	EARLY BIRD	-29.83	MAR – APR '66	-1.527 ±0.015	-1.546	-1.522	$-1.496^{2\sigma}$	$-1.441^{7\sigma}$
12-4	EARLY BIRD	-31.29	JAN – MAR '66	-1.644 ±0.012	-1.651	$-1.617^{2\sigma}$	$-1.585^{4\sigma}$	$-1.540^{9\sigma}$
12-5	EARLY BIRD	-28.83	APR – MAY '66	-1.494 ±0.012	-1.472	$-1.455^{3\sigma}$	$-1.432^{5\sigma}$	$-1.370^{8\sigma}$

* THESE ARE THE LONGITUDES NEAR THE MID POINTS OF THE DRIFT ARCS, WHERE THE ACCELERATION IS BEST DETERMINED BY THE DATA (SEE REFERENCE [4] AND APPENDIX A FOR THE LONGITUDE SPAN COVERED IN EACH DATA ARC).

** ADJUSTED DATA FOR LIKELY SUN-MOON-EARTH MODEL BIAS (SEE TABLE 1).

Table 4

Low Order Longitude Gravity Harmonics From Recent Investigations

	10^6C_{22}	10^6S_{22}	10^6C_{31}	10^6S_{31}	10^6C_{32}	10^6S_{32}	10^6C_{33}	10^6S_{33}	10^6C_{42}	10^6S_{42}	10^6C_{44}	10^6S_{44}
(1) KAULA 1966a	1.56	-0.88	1.93	0.19	0.27	-0.26	0.079	0.198	0.067	0.134	-0.0013	0.0068
(2) KAULA 1966b	1.57	-0.90	2.10	0.16	0.25	-0.27	0.077	0.173	0.074	0.159	-0.0066	0.0023
(3) SAO 1966	1.54	-0.87	2.09	0.29	0.25	-0.18	0.078	0.226	0.074	0.148	-0.0011	0.0049
(4) ANDERLE 1965	1.58	-0.98	2.32	0.30	0.33	-0.31	0.082	0.227	0.061	0.150	-0.0087	0.0071
(5) GUIER & NEWTON '65	1.54	-0.77	1.99	0.23	0.42	-0.23	0.092	0.137	0.094	0.098	-0.0044	0.0040
(6) WAGNER 1966	1.56	-0.93	-1.4	-0.3			0.045	0.165				
(7) WAGNER 1967a	1.56	-0.93			0.25	-0.19					-0.0090	0.0070
(8) IZSAK 1965	1.34	-0.81	1.73	-0.04	0.13	-0.27	-0.024	0.195	0.045	0.130	-0.0023	0.0091
(9) WAGNER 1967b	1.55	-0.915	0.3	-1.5			0.03	0.155				

	10^6J_{22}	λ_{22}	10^6J_{31}	λ_{31}			10^6J_{33}	λ_{33}	10^6J_{42}	λ_{42}	10^6J_{44}	λ_{44}
(1) KAULA 1966a	1.79	-14.7°	1.94	5.6°			0.213	22.8°	0.150	31.6°	0.0069	25.2°
(3) SAO 1966	1.77	-14.7	2.11	8.0			0.239	23.7	0.165	31.6	0.0050	25.6
(4) ANDERLE 1965	1.86	-15.9	2.34	7.4			0.242	23.4	0.162	33.9	0.0112	35.2
(9) WAGNER 1967b	1.80	-15.3	1.53	-79.0			0.158	26.4				

REFERENCES
(1) KAULA 1966a, "TESTS AND COMBINATION OF SATELLITE DETERMINATIONS OF THE GRAVITY FIELD WITH GRAVIMERY," JOURNAL OF GEOPHYS RES, 71, 5303 (1966).
(2) KAULA 1966b, "TESSERAL HARMONICS OF THE EARTH'S GRAVITATIONAL FIELD FROM CAMERA TRACKING OF SATELLITES," JOURNAL OF GEOPHYS RES. 71. 4377 (1966).
(3) SAO 1966, E.M. GAPOSHKIN'S PAPER, "A DYNAMICAL SOLUTION FOR THE TESSERAL HARMONICS OF THE GEOPOTENTIAL AND STATION COORDINATES USING BAKER-NUNN DATA," SMITHSONIAN ASTROPHYSICAL OBSERVATORY, CAMB, MASS, MAY 1966.
(4) ANDERLE 1965, "DETERMINATION OF THE EARTH'S GEOID BY SATELLITE OBSERVATIONS," REPORT #2027, NAVAL WEAPONS LABORATORY, DAHLGREN, VIRGINIA, MARCH 1966.
(5) GUIER AND NEWTON 1965, QUOTED IN REFERENCE (1) ABOVE.
(6) WAGNER 1966, "LONGITUDE VARIATIONS IN THE EARTH'S GRAVITY FIELD AS SENSED BY THE DRIFT OF THREE SYNCHRONOUS SATELLITES," J. GEOPHYS RES, 71, 1703 (1966).
(7) WAGNER 1967a, "LONGITUDE VARIATIONS IN THE EARTH'S GRAVITY FIELD AS SENSED BY TWO RUSSIAN 12 HOUR SATELLITES," J. GEOPHYS RES, IN PRESS, 1967.
(8) IZSAK 1965, "A NEW DETERMINATION OF NON ZONAL HARMONICS BY SATELLITES," IN: TRAJECTORIES OF ARTIFICIAL CELESTIAL BODIES, PUB., SPRINGER VERLAG, NEW YORK, 1966.
(9) WAGNER 1967b, BEST RESULTS OF THIS REPORT, SEE TABLE 2.

APPENDIX A
Basic Data

In this appendix I list the basic data used in this gravity analysis. Except for Early Bird, the data consists mainly of sets of cartesian and spherical coordinate ("ADVARB") vectors, or mean Keplerian elements for the Syncom satellites 2 and 3, reduced from primary range and range rate and minitrack observations. The Data Systems and Tracking Directorate at Goddard Space Flight Center (through the offices of Dr. Joseph Siry) supplied both cartesian and mean element sets and related equator crossing data (at near epoch times) for Syncoms 2 and 3 from August 1963 through the spring of 1965. Subsequently, the Airforce Systems Command at Sunnyvale, California has been supplying "ADVARB" vector elements and near epoch time crossing data for Syncoms 2 and 3.

The Early Bird data listed here consists mainly of equator crossing longitudes for the period April 1965 to May 1966, estimated directly from range, azimuth and elevation measurements near the crossings, taken from Comsat's tracking facility at Andover, Maine.

Table A1, repeated for completeness from Reference [4], gives the GSFC vector elements for data Arcs 1 through 5. The analysis of these elements, resulting in the reduced accelerations listed for Arcs 1, 2, 4, 5-1, and 5-2 in Table 1, has been adequately described in Reference [4]. (Arc 5-1 here was called Arc 5A in Ref. [4], and Arc 5-2 was called Arc 5-18.) Table A2 gives the same kind of data, already analyzed, for Arcs 6, 7 and 8. The results of the analysis of data Arc 8 in Table A2, is listed in Table 1 as Arc 8-1.

In Tables A3 and A4 I list the mean semimajor axis and related data for Syncoms 2 and 3, also reported by the GSFC Tracking Directorate which I have used to calculate additional, independently observed accelerations for data arcs: 8-1a (slow drift), 8-2 (slow drift) 8-2a (slow drift), 1a (slow drift), 2a (slow drift), 4a (fast drift), 6a (slow drift), and 7a (slow drift). The accelerations in Arcs 6a and 7a were too poorly determined to be useful in the gravity analysis and are not reported in Table 1. The best acceleration results for arcs 8-1a, 8-2, 8-2a, 1a, 2a and 4a <u>are</u> reported in Table 1.

In Table A5 I list the mean semimajor axis and related GSFC reported data in the fast drift Arc 5 (Syncom 2). The single, best observed acceleration found from this data is reported as data Arc 5a in Table 1.

In Table A6 is listed tracking data for the "broken" arc 10 (Syncom 3). The best acceleration results for this slow drift arc are reported in Table 1 as data arcs 10 and 10a, though only the equator crossing analysis gave sufficiently small residuals to be useful for the gravity solutions.

In Table A7 is listed a set of Department of Defense (DOD) elements, computed at Sunnyvale, California, from the spring of 1965 to January 1967. These vector elements (ADVARB) were computed from range and range rate tracking at Stations in Hawaii, the Phillipines, Vietnam and Africa. The earth model used to reduce the tracking data to these vector elements was more complex than that used to derive the GSFC elements. However, the accuracy of these elements when derived from information over a few revolutions, are not superior to the GSFC elements because of this, due to the very small short term effects of the more sophisticated model on the high altitude 24 hour satellites. Since the data used to derive the bulk of elements spans no more than a one week period, even the long term (resonance) effects of the longitude gravity model used, are relatively small. However, the earth model used by DOD, Sunnyvale, since the spring of 1966 has incorporated the gravity harmonics reported in Reference [4] and has resulted, on average, in better elements when the data span used is greater than about a week.

These DOD elements have the following definition: Epoch, Date (Universal Time): M = month, D = day, Y = year, H = hour, MI = minute, S = second: α° = right ascension of the satellite with respect to the vernal equinox at epoch (degrees), δ° = declination with respect to the equator at epoch (degrees), β° = flight path angle from the satellite's outward geocentric radius vector to the velocity vector (degrees), AZ° = azimuth or the angle (from north clockwise) between the planes formed by the satellite's geocentric radius and the earth's north pole vectors and the satellite's radius and velocity vectors (degrees), RAD' = the satellite's distance (radius) to the center of mass of the earth (feet), V/FPS = the satellite's velocity in feet per second. The sets of DOD elements applicable to the long free arcs 8-3 to 8-5, 11, and 13 are shown in Tables A7 and A8. Additional information from these and other orbits, used in the long term acceleration analysis for these slow drift arcs, are shown in Tables A9, A10 and A11. The best acceleration results for these arcs are listed in Table 1.

Finally, in Table A12 is listed the ascending and descending equator crossings for Early Bird in Arcs 9 and 12, as estimated directly from near-crossing range azimuth and elevation observations (supplied by the COMSAT Corporation) taken at the Andover, Maine tracking station. Also listed are occasional osculating (vector) Keplerian elements for Early Bird, determined from the full set of Andover Tracking data over a number of revolutions past the orbit date. The best acceleration results from these slow drift arcs are shown in Table 1. The data-arc time spans (as for all the acceleration points) appear in Table 3.

Table A1

Inertial Position and Velocity Coordinates for Syncom 2 and Syncom 3 as Reported by GSFC*

	Tracking Epoch (Yr-mo-day-hr-min UT)	X (10^4 km)	Y (10^4 km)	Z (10^4 km)	$\dot{X}$ (km/sec)	$\dot{Y}$ (km/sec)	$\dot{Z}$ (km/sec)
	63-8-18-1-30.0	1.8517253	-3.6656408	-0.95346425	2.5197630	0.87570544	1.5296730
	63-8-22-6-12.14	3.8192813	0.19653916	1.7732339	-0.64139671	2.8111679	1.0698498
	63-8-26-17.0	-3.9190365	0.71434463	-1.3838910	-0.030659063	-2.7659652	-1.3414586
	63-8-31.0	1.2517473	-3.8173186	-1.2805028	2.7082374	0.42130417	1.3937010
	63-9-3-13-23.0	-2.6683093	3.2430659	0.37724660	-2.0920997	-1.5282086	-1.6556391
	63-9-5.0	1.5690433	-3.7540418	-1.1058861	2.6179496	0.66119258	1.4710835
	63-9-9.0	1.8101775	-3.6842867	-0.96169979	2.5333080	0.84735057	1.5232783
	63-9-12-2.0	3.4100141	-2.4566117	0.33394973	1.4036497	2.1745471	1.6606540
	63-9-17-2.0	3.5605032	-2.1949356	0.52762629	1.1881299	2.3199229	1.6320863
Arc 1	63-9-20-2.0	3.6381029	-2.0310580	0.64240062	1.0551433	2.3993342	1.6084890
	63-9-27-2.0	3.7828113	-1.6282253	0.90343513	0.73324914	2.5577582	1.5413518
	63-10-1-2.0	3.8398851	-1.3915057	1.0449696	0.54792106	2.6322531	1.4928190
	63-10-8-2.0	3.8997221	-0.96844341	1.2765410	0.22281006	2.7325580	1.3929604
	63-10-14-2.0	3.9114166	-0.59213158	1.4569605	-0.059266662	2.7895298	1.2936179
	63-10-22-2.0	3.8655564	-0.089237507	1.6821569	-0.43011588	2.8231687	1.1399466
	63-10-30.0	3.7935711	-1.5763511	0.94831895	0.69205550	2.5804974	1.5229227
	63-11-6.0	3.8724273	-1.1762815	1.1818209	0.38097748	2.6938419	1.4335987
	63-11-12-5.0	1.1446010	3.4554430	2.1294725	-2.7244144	1.2840822	-0.61733366
	63-11-18-13.0	-3.7038702	-0.58064695	-1.9332132	0.90759960	-2.7961257	-0.89794623
	63-11-28-1.0	3.4781437	1.1376687	2.0944723	-1.2933144	2.7059520	0.67780023
	63-12-4.0	3.7151749	0.53514140	1.9201218	-0.87415171	2.8043813	0.90960269
	63-12-10.0	3.5731662	0.92615699	2.0379487	-1.1461780	2.7500585	0.76033287
	63-12-16-17.0	1.0227024	-3.8691081	-1.3292554	2.7458357	0.25931246	1.3585847
	63-12-23-19.0	3.0804533	-2.8787714	0.055186822	1.7485346	1.9038213	1.6650503
	64-1-6-17.0	2.2436953	-3.5177574	-0.60704656	2.3262615	1.2062956	1.6089899
	64-1-9-6.0	-3.0926247	2.8665793	-0.080953346	-1.7324029	-1.9159081	-1.6667974
Arc 2	64-1-15-18.0	3.3299438	-2.5658898	0.32807382	1.4797710	2.1321920	1.6489369
	64-1-20-21.0	3.7030072	0.56000451	1.9369923	-0.88759725	2.8080493	0.88485319
	64-1-29-20.0	3.8204264	0.093177361	1.7811029	-0.55721471	2.8372181	1.0470801
	64-2-5-16.0	2.8698222	-3.0876991	-0.10282631	1.9209748	1.7308532	1.6640514
	64-2-10-19.0	3.8650196	-0.19769561	1.6738813	-0.34675337	2.8365031	1.1356011
	64-2-17-17.0	3.7268026	-1.7536007	0.90292256	0.82362190	2.5381818	1.5281483
	64-2-25-19.0	3.6533259	0.69908427	1.9851452	-0.98120516	2.7965023	0.82109998
	64-3-4-23.0	0.18113658	3.8087583	1.8019013	-2.8347353	0.61701878	-1.0178939
	64-3-10-13.0	2.0644779	-3.6124046	-0.68632246	2.4052556	1.0737921	1.5862758
	64-3-18-3.0	-3.6249117	2.0233288	-0.74902788	-1.0365741	-2.4353607	-1.5693664
	64-3-24-13.0	2.3283566	-3.4999056	-0.50715805	2.2721038	1.2746548	1.6158241
Arc 3	64-4-1-22.0	0.76296064	3.6490419	1.9857054	-2.7806607	1.0205339	-0.81923611
	64-4-7-15.0	3.4461234	-2.4088100	0.50885287	1.3277141	2.2415368	1.6144312
	64-4-13-19.0	3.3872421	1.3385265	2.1522760	-1.4069923	2.6725021	0.54080057
	64-4-25-2.0	-2.5603443	3.3390780	0.29994066	-2.1318214	-1.4887792	-1.6428786
	64-4-28-15.0	3.2628949	-2.6693162	0.32101150	1.5457882	2.0856009	1.6366277
	64-5-5-16.0	3.7257132	-1.7632128	0.94048572	0.82412264	2.5449717	1.5038900
	64-5-12-16.0	3.7475309	-1.6867283	0.99296812	0.76273664	2.5725322	1.4891387
Arc 4	64-5-19-14.0	2.7849331	-3.1784434	-0.10945226	1.9747957	1.6719452	1.6505955
	64-5-25-15.0	3.4307022	-2.4126224	0.53392194	1.3319460	2.2493385	1.6072617
	64-6-2-21.0	1.7406646	3.1597779	2.1946670	-2.5288299	1.6899106	-0.43439828
	64-6-9-21.0	1.6500071	3.2194181	2.1774956	-2.5601432	1.6304633	-0.47782909
	64-6-16-15.0	3.5655116	-2.1536100	0.72108034	1.1248629	2.3871212	1.5668312
	64-6-23-15.0	3.6075927	-2.0587512	0.78733380	1.0494437	2.4320607	1.5495642
	64-7-4-2.0	-3.2093967	2.7165420	-0.32063943	-1.5841089	-2.0660850	-1.6378223
	64-7-7-3.0	-3.6954496	1.7950587	-0.94983861	-0.85046154	-2.5458831	-1.5023067
	64-7-13-17.0	3.7354217	0.41539202	1.9259618	-0.76727529	2.8431082	0.87209834
	64-7-21-21.0	0.68011374	3.6978808	1.9157389	-2.7798310	-0.96706741	-0.88586596
	64-7-27-16.0	3.8417868	-0.11824881	1.7510381	-0.39126192	2.8593634	1.0493355
	64-8-3-17.0	3.4664817	1.1480683	2.1210692	-1.2649191	2.7375684	0.58214636
	64-8-11-1.0	-3.3701691	2.4805650	-0.51870386	-1.3894809	-2.2250586	-1.6062097
	64-8-17-19.0	1.6959231	3.2024028	2.1645995	-2.5377008	1.6647695	-0.48003497
	64-8-25-10.0	1.5330007	-3.8258893	-0.91436182	2.5905352	0.67495556	1.5073075
	64-9-1-10.0	1.7622665	-3.7590544	-0.76800569	2.5108491	0.85857627	1.5478150
	64-9-9-14.0	3.8729406	-0.56806750	1.5864037	-0.064200095	2.8378419	1.1715632
	64-9-15-12.0	3.4973065	-2.2642849	0.69291203	1.2114165	2.3483095	1.5648130
	64-9-22-10.0	2.3957332	-3.4619283	-0.32713684	2.2142000	1.3764322	1.6238887
Arc 5	64-9-29-6.0	-1.2057564	-3.4918173	-2.0387967	2.6768512	-1.3377786	0.70292893
	64-10-6-5.0	-1.9027758	-3.0642587	-2.1871975	2.4522966	-1.8112966	0.39976832
	64-10-13.0	-3.7909750	1.3890374	-1.2159474	-0.54220619	-2.6929405	-1.3843106
	64-10-20-16.0	2.3418688	2.7061755	2.2406431	-2.2408225	2.0926322	-0.18928830
	64-10-26-16.0	2.1737218	2.8588045	2.2200917	-2.3278640	1.9849102	-0.28044993
	64-11-2-5.0	-1.0575392	-3.5703165	-1.9843669	2.7067256	-1.2347065	0.77366371
	64-11-11-2.0	-3.2269498	-1.5931919	-2.1991397	1.5433675	-2.6360297	-0.35716605
	64-11-17-6.0	0.44169064	-3.9493268	-1.4227193	2.7947443	-0.14738721	1.2691720
	65-1-10-6.0	1.8733482	-3.7329199	-0.61394837	2.4551255	0.97133874	1.5716495
	65-1-13-16.0	-0.024904471	3.9169200	1.5734233	-2.8064159	0.44943751	-1.1686893
	65-1-20-12.0	3.2361444	1.5906403	2.1989944	-1.5260383	2.6448765	0.33028481
	65-1-27-4-5.0	0.42866892	-3.9652039	-1.3910958	2.7914381	-0.14522612	1.2721610
	65-2-2-13-30.0**	1.8326846	3.1377111	2.1684747	-2.4504221	1.7730384	-0.49949115
	65-2-16-4-5.0	0.94696655	-3.9573969	-1.1249388	2.7174166	0.24662704	1.4128023

*From the Data Systems and Tracking Directorate, computed from range and range rate and Minitrack Data by Robert Chaplick, Gerald Repass, and Carleton Carver, from an orbit determination program due to Dr. Joseph Siry (see text in Appendix A of Reference [4] for earth-gravity constants used in this program.) The inertial orthogonal system x, y, z has the x axis pointing towards the vernal equinox of epoch and the z axis pointing towards the North Celestial Pole.

**This orbit gave unacceptably large residuals in the acceleration analysis in Section 1 and was consequently ignored there in the final reduction of arc 5 data.

Table A2

Inertial Position and Velocity Coordinates or Mean Elements for Syncom 2 and Syncom 3 as Reported by GSFC*

Arc	Tracking Epoch (yr-mo-day-hr-min UT)	x (10^4 km)	y (10^4 km)	z (10^4 km)	$\dot{x}$ (km/sec)	$\dot{y}$ (km/sec)	$\dot{z}$ (km/sec)	Semimajor Axis (earth radii)	Eccentricity	Inclination (degrees)	Mean Anomaly (degrees)	Argument of Perigee (degrees)	Right Ascension of the Ascending Node (degrees)
Arc 6	64-10-31-2.0	-1.4631983	-3.9552279	0.0044875382	2.8832439	-1.0673281	0.0040784579						
	64-11-3-13-18.0	1.9559545	3.7357796	-0.0046653417	-2.7240257	1.4261328	0.0010170648						
	64-11-7-8.0	4.0979330	-0.99735096	0.000090583545	0.72682785	2.9870550	-0.0031209910						
	64-11-16-3.0	0.69358189	-4.1594677	0.0003877877	3.0328345	0.50550362	-0.0020335351						
	64-11-24-3.0	1.2284361	-4.0339231	0.00056889501	2.9413798	0.89560376	-0.0041770365						
	64-11-30-10-35.0	2.8977682	3.0637592	-0.002529583	-2.2336845	2.1126627	0.0044895056						
	64-12-8-12-45.0	0.23956950	4.2107011	0.010288296	-3.0691699	0.17465649	0.011725721						
	64-12-15-12.0	0.57474705	4.1777703	0.0011544263	-3.0457305	0.41900501	0.0066359655						
	64-12-21-9.0	3.0948417	2.8634925	-0.0059212736	-2.0882709	2.2570007	0.010048741						
Arc 7	65-1-14-23.5	1.2675646	-4.0179928	-0.051959215	2.9359926	0.92060244	-0.047842619						
	65-1-30-13-10.0	-3.4792181	2.3828935	-0.0058904292	-1.736821	-2.5371972	-0.0083528082						
	65-2-2-6.0	3.2099039	2.7368950	0.0073851190	-1.9943285	2.3390669	0.0012901180						
	65-2-9-11.0	-2.2119906	3.5906580	-0.0049486959	-2.6173528	-1.6131485	-0.0081798989						
	65-2-16-12.0	-3.3564297	2.5533931	-0.0042520595	-1.8613403	-2.4471176	-0.0086970709						
	65-2-23.0	3.5938828	-2.2084394	0.0096558595	1.6094139	2.6188512	0.0026358856						
	65-3-2.0	3.8120235	-1.8069874	0.015075846	1.3165671	2.7773230	-0.00057799012						
	65-3-9.0	3.9810232	-1.3940918	0.0045517934	1.0162757	2.9011202	0.0024674641						
	65-3-16.0	4.1104734	-0.95605039	0.026135089	0.69589465	2.9925915	-0.00060597968						
Arc 8	65-2-25.0	-2.6260533	-2.4306852	-2.2283266	2.0528730	-2.2888731	0.081154582						
	65-3-3.0	-2.3397165	-2.7254249	-2.2051595	2.2300224	-2.1051269	0.23910311						
	65-3-6.0							6.6112847	.00076	31.939	308.359	333.048	309.370
	65-3-13.0							6.6113429	.00069	31.912	326.845	321.447	309.095
	65-3-29.0	-0.85799562	-3.6815475	-1.8631946	2.7341821	-1.0890101	0.89574242						
	65-4-5.0							6.6111445	.00069	31.830	329.612	340.634	308.896
	65-4-12.0							6.6111335	.00073	31.848	328.269	348.585	308.947
	65-4-19.0							6.6110585	.00065	31.867	353.146	330.838	308.586
	65-4-26.0							6.6110267	.00063	31.787	353.717	337.005	308.580
	65-5-3.0							6.6110035	.00061	31.807	359.897	337.757	308.417
	65-5-10.0							6.6109407	.00059	31.731	0.012	344.515	308.335

*From the Data Systems and Tracking Directorate (see note in Table A1). The mean elements, good for more than one orbit (smoothing out the periodic sun, moon, and zonal gravity effects) are calculated from the vector elements of position and velocity according to a theory due to D. Brouwer.

Table A3

Mean Elements and Related Data for Syncom 2 in Arc 8, As Reported By GSFC

Orbit, 8-	Tracking Epoch: (Yr-Mo-Day-Hr-Min: U.T.)	Semimajor Axis (a): Earth Radii	Estimated σ(a): (10^{-6} E.R.)	(Asc. Eq. Crossing Data) Time: From 1965.0 (Days)	Time From Jan. 109.0997, 1965 (Sid. Days)	λ (Ascending Eq. Cross.) Deg's	Inclination i (Deg's)	Mean Anomaly MA (Deg's)	Arg. of Perigee ω (Deg's)	R.A. of The Asc. Node β (Deg's)	Eccentri-City e (10^{-5})	(Descending Eq. Crossing Data) λ (Descending Eq. Cross.) Deg's.	Time: (Yr-Mo-Day-Hr-Min-Sec, U.T.)	Time From 65-5-3-13-27-15.5:Sid. Days
1	65-2-24-19-30.0	6.6110989	1.650	56.24										
1a	65-2-25.0	3906	.755	56.2412	-53	67.733	31.956							
2	65-3-3.0	6.6109100	13.3	62.2257	-47	.423	.930							
3	65-3-6.0	6.6112847	1.680	65.2177	-44	.270	.939							
4	65-3-13.0	3429		72.1986	-37	.007	.912							
5	65-3-29.0	1906	7.22	88.1567	-21	66.314	.955							
6	65-4-5.0	1446	1.45	95.1378	-14	.071	.830					66.023	65-4-5-15-16-37.1	-28
7	65-4-12.0	1335	1.70	102.1195	-7	65.822	.848					65.794	65-4-12-14-50-12.8	-21
8	65-4-19.0	0585	0.567	109.0997	0	.712	.867					65.647	65-4-19-14-21-50.3	-14
9	65-4-26.0	0267	.810	116.0811	7	.534	.787					65.4895	65-4-26-13-54-55.1	-7
10	65-5-3.0	0035	4.51	123.0619	14	.404	.807					65.362	65-5-3-13-27-15.5	0
11	65-5-10.0	6.6109407	1.63	130.0428	21	.288	.731					65-265	65-5-10-12-59-47.7	7
12	65-5-17.0	8998	2.97	137.0238	28	.244	31.820	15.179	336.214	308.312	63	65.200	65-5-17-12-32-26.3	14
13	65-5-24.0	8153	1.67	144.0046	35	.155	.717	13.186	345.151	308.192	53	65.141	65-5-24-12-4-40.5	21
14	65-5-31.0	7771	7.66	151.9820	43	.1895	.725	30.730	334.768	307.954	51	65.1575	65-5-31-11-8-13.5	28
15	65-6-7.0	7276	2.09	158.9626	50	.217	.727	35.182	337.312	307.882	56	65.183	65-6-7-11-8-13.5	35
		Avg: Orbits 8-6/8-15: a = 6.610953 Avg: Orbits 8-7/8-15 a = 6.610931					Avg: Orbits 8-6/8-15: i = 31.786 Avg: Orbits 8-7/8-15 i = 31.780							

Data Arc Analyses

Arc 8-1 Analyses the Ascending Equator Crossing data from orbits 8-1 through 8-10 (slow drift)

Arc 8-1a Analyses the Semimajor Axis data from orbits 8-1 through 8-9 (slow drift)

Arc 8-2 Analyses the Descending Equator Crossing data from orbits 8-6 through 8-15 (slow drift)

Arch 8 -2a Analyses the Semimajor Axis Data from orbits 8-7 through 8-15 (slow drift)

See Table 1 for best results of these analyses.

Table A4

Mean Elements And Related Data for Syncoms 2 and 3 In Arcs 1, 2, 4, 6 and 7, as Reported By GSFC

Orbit, 4-	Epoch (Yr-Mo-Day-Hr, U.T.)	Mean a (E.R.)	$\dot{\lambda}$ † (°/Sid. Day)	Long. of First Asc. Eq. Cross Past Epoch λ (Deg's)	Estimated σ(a): (10^{-6} E.R.)	$\dot{\lambda}$ † (°/Sol. Day)
1	64-4-25-2.0	6.6207968	-0.83133	-117.18	101.000	-0.8336
2	28-15.0	7372	2646	-120.43	0.568	287
3	5-5-16.0	6083	1593	-126.09	.487	182
4	12-16.0	4847	0583	-131.74	.471	080
5	19-14.0	4508	0306	-136.49	.847	053
6	25-15.0	4267	0109	-142.02	.849	033
7	6-2-21.0	2806	-0.78916	-148.245	1.850	-0.7913
8	9-21.0	1266	7658	-153.64	1.360	787
9	16-15.0	9188	5961	-158.96	1.020	617
10	23-15.0	8803	5646	-164.22	0.805	585

† Estimated from mean a data

Orbit, 6-	Epoch (Yr-Mo-Day Hr-min, U.T.)	Mean a (E.R.)	Estimated σ(a): (10^{-6} E.R.)	Time* From 1964.0, (Days)	Long. of First Asc. Eq. Cross After Epoch: λ (Deg's)	Time From Jan. 329.6393,1964 (Sid. Days)
1	64-10-31-2.0	6.6116368	1.420	305.9723	180.219	-24
2	64-11-3-13-18.0	8412	1.060	8.7567	.028	-21
3	64-11-7-8.0	6799	0.229	12.8308	179.737	-17
4	64-11-16-3.0	6059	.595	21.6437	.191	-8
5	64-11-24-3.0	5200	1.420	29.6393	178.798	0
6	64-11-30-10-35.0	5101	1.940	35.5028	.509	6
7	64-12-8-12-45.0	3451	1.130	44.4400	.171	15
8	64-12-15-12.0	2252	1.670	51.4760	177.968	22
9	64-12-21-19.0	6.6108940	125.000	356.4394	.814	27

Orbit, 1-	Epoch (Yr-Mo-Day-Hr, U.T.)	Time in Days From 63-8-68.495*	Mean a (E.R.)
1	(See Table 1, NASA TN-D-3557)	-50.365	6.6105202/6.6104741
2		-45.379	05391
3		-41.390	298
4		-37.401	7646
5		-32.415	979
6		-28.427	8160
7		-24.438	472
8		-19.451	702
9		-16.459	9835
10		-9.478	6.6112494/6.6109979
11		-5.489	126
12		1.492	543
13		7.477	3540
14		15.455	6250
15		23.435	5592
16		30.416	7250
17		36.402	815
18		42.386	6.6120076

*Time at first ascending equator crossing past the epoch.

Orbit, 7-	Epoch (Yr-Mo-Day-Hr-Min, U.T.)	Mean a (E.R.)	Estimated σ(a): (10^{-6} E.R.)	Time* From 1965.0 (Days)
1	65-1-14-23-30.0	6.6123299	2.410	15.0855
1A	65-1-22-2.0	5707	1.150	23.0
2	65-1-30-13-10.0	3134	1.330	20.9720
3	65-2-2-6.0	5066	0.453	34.0364
4	65-2-9-11.0	3760	0.561	40.8915
5	65-2-16-12.0	3509		47.7895
6	65-2-23.0	2057	0.682	54.8054
7	65-3-2.0	3565	0.473	61.732
8	65-3-9.0	2508	0.495	68.8539
9	65-3-16.0	5657		75.7421

Orbit, 2-	Epoch	Time, In Days From 77.729 Nov. 1963*	Mean a (E.R.)
1	(See Table 2, NASA TN-D-3557)	-48.873	6.6107434
2		-42.890	9495
3		-36.906	462
4		-30.923	6.6111018
5		-22.944	0200
6		-9.978	763
7		-6.986	6.6113726
8		-0.005	6256
9		4.982	130
10		13.961	879
11		19.945	6.6118417
12		25.930	9067
13		32.912	6.6121556
14		40.893	0819
15		48.873	3652
16		53.861	3870

Table A5

Mean Elements and Related Data for Syncom 2, Arc 5, as Reported by GSFC

Orbit # 5-	Tracking Epoch (See Ref. [4])	Mean Semimajor Axis, a : (Earth Radii)	$\dot{\lambda}^{\dagger}$ (°/Sid.Day)	i Inclination (Rad.)	λ (First Asc. Eq. Cross. Past Epoch) Deg's	Est. $\sigma(a)$: (10^{-5} E.R.)	$\dot{\lambda}^{\dagger}$ (°/Sol. Day)
1	64-7-4-2.0	6.6165547	-0.48480	.56794437	-171.26	.5440	-.4861
2	64-7-7-3.0	6.6166962	9636	.56787141	-172.70	.0920	977
3	64-7-13-17.0	6.6165633	8551	.56726514	-176.04	.0418	868
4	64-7-21-21.0	4925	7972	50460	-179.79	.1040	810
5	64-7-27-16.0	4312	7471	26786	177.41	.0610	760
6	64-8-3-17.0	3966	7189	.56681234	174.18	.0623	732
7	64-8-11-1.0	3059	6448	.56628775	171.00	.0683	658
8	64-8-17-19.0	3334	6673	563818	167.86	.105	680
9	64-8-25-10.0	2740	6187	624261	164.69	.370	631
10	64-9-1-10.0	3147	6520	543507	161.57	.129	665
11	64-9-9-14.0	1847	5458	00697	157.51	.168	558
12	64-9-15-12.0	3284	6632	481867	154.82	.118	676
13	64-9-22-10.0	2871	6294	377349	152.09	.179	642
14	64-9-29-6.0	4662	7757	420689	148.87	.140	789
15	64-10-6-5.0	4894	7947	09826	145.70	.152	808
16	64-10-13.0	5676	8586	394443	142.39	.295	872
17	64-10-20-16.0	5779	8670	55395	138.60	.300	880
18	64-10-26-16.0	8624	-0.50994	289186	135.72	.310	-.5113
19	64-11-2-5.0	5241	-0.48230	4154	132.71	.620	-.4836
20	64-11-11-2.0	9057	-0.51347	352303	128.11	.203	-.5149
21	64-11-17-6.0	9383	1614	250948	125.37	.225	176
22	65-1-10-6.0	6.6172930	4511	078882	94.73	.291	466
23	65-1-13-16.0	6.6182227	2106	135396	92.46	.383	-.6228
24	65-1-20-12.0	2444	2283	059344	88.16	.180	245
25	65-1-27-4-5.0	2762	2543	.55772198	84.09	.560	271
26	65-2-2-13-30.0	4470	3938	.53948234	81.59	.945	411
27	65-2-16-4-5.0	0976	1084	.56045061	72.25	1.260	125
	Avg:	6.616855		Avg: 32.33°			
	Use:	a = 6.6169		Use i = 32.3°			

† Estimated from Mean a data.

Table A6

Mean Elements and Related Data for Syncom 3 in Arc 10, as Reported by GSFC

Tracking Epoch Time: 1965	Mean a (Earth Rad.)	Est. $\sigma(a)$: (10^{-6} E. R.)	Time: Days From 26 April '65	Asc. Eq. Cross. Long., λ, (Deg's)
29 March	6.610205	0.995	-28	171.768
5 April	122	1.05	-21	172.151
12 April	186	1.80	-14	.561
19 April	133	1.78	-7	173.009
26 April	68	4.17	0	173.484
Orbit Maneuver				
3 May	6.611256	2.84	7	173.553
10 May	303	.858	14	.360
17 May	178	4.32	21	.172
24 May	027	5.05	28	.028
31 May			35	172.558

Table A7

Syncom Vector Elements as Reported by DOD, Air Force Systems Command

Syncom 2														
Date (U.T.)*						α°	δ°	β°	AZ°	RAD'	V/FPS			
M	D	Y	H	MI	S									
2	20	65	0	0	0	219.4469910	-32.0060846	89.9961150	90.0523824	138394502.9	10087.10240			
2	25	65	0	0	0	222.7701816	-31.9443252	90.031929	88.2550560	138293096.3	10090.69733			
2	28	65	0	0	0	226.1018567	-31.7785108	90.0344592	86.4741062	138298766.5	10090.45195			
3	10	65	0	0	0	236.9487701	-30.6899438	90.0357632	80.8231253	138300633.3	10090.46319			
3	29	65	0	0	0	256.8546943	-26.1592716	90.0241538	71.1025156	138274034.5	10092.17478			
7	7	65	10	10	0.0	141.0073731	-8.2174429	90.0186946	120.732494	138393044.4	10082.99860			
7	14	65	0	0	0.0	352.9294622	23.7735710	89.9682102	68.3979102	138309521.8	10088.94775			
7	21	65	2	56	0.0	50.6909182	30.9370813	89.9755377	96.9760624	138374666.0	10084.28522			
8	4	65	2	56	0.0	66.8402089	28.1971360	89.9732606	105.0415528	138301348.0	10083.76856			
8	13	65	19	55	0.0	324.9107377	10.6807965	89.9766084	60.0492779	138262458.4	10092.53995	Arc 8-3		
9	2	65	3	25	0	103.7197146	+13.4161276	89.99819390	118.8636917	138399442.9	10082.32194			
9	25	65	2	56	0.0	118.3718539	4.8599594	90.0149413	121.1787151	138404548.1	10081.78149			
10	14	65	11	49	47.836	274.9555001	-17.5750405	90.0112478	63.5003952	138237213.7	10094.02949			
10	31	65	12	1	38.392	293.8988897	-7.1864926	89.9856550	59.2701607	138214886.9	10095.66179			
11	10	65	9	58	4.947	275.6513998	-17.0126842	89.9999990	63.1174356	138199480.8	10096.73402			
11	23	65	9	11	46.283	277.6633809	-15.904909	89.9999972	62.5127121	138200461.1	10096.65478			
12	22	65	7	28	42.978	282.2031934	-13.2876472	90.0022143	61.3126206	138199843.2	10096.78530			
1	6	66	6	42	17.953	286.0163485	-11.1194454	90.0075717	60.5651416	138200010.1	10096.88668		Arc 8-4	
1	20	66	6	19	13.304	294.0064632	-6.4105872	89.9993862	59.3237703	138199372.6	10096.86378			Arc 8-5
2	4	66	5	14	14.653	296.2184957	-4.9860918	90.0064450	59.1887599	138198691.4	10096.94630			
3	4	66	3	39	42.440	298.7955599	-3.2509379	90.0003232	58.9696426	138191420.0	10097.82936			
3	18	66	2	35	48.364	297.6499252	-3.8163274	90.0004623	59.0716091	138199006.9	10096.97391			
3	31	66	1	48	14.959	298.9785137	-2.7767197	90.0014741	58.9964413	138205974.3	10096.52221			
4	11	66	1	0	28.001	298.4887986	-2.9501216	90.0002953	59.0361118	138219728.3	10095.49430			
5	3	66	23	42	9.609	301.9673741	-6.6805596	90.0001197	58.9685272	138218816.9	10095.49430			
5	10	66	23	0	31.848	299.1548163	-2.3482622	90.0004991	59.0544324	138219975.8	10095.67965			
5	17	66	22	38	9.857	300.4472863	-1.4783249	89.9996532	59.0178444	138229437.6	10094.82327			
6	1	66	21	34	45.440	299.7758944	-1.6984681	89.9992706	59.0349305	138233565.3	10094.61720			
7	1	66	19	13	34.208	295.0250382	-4.2796550	89.9991824	59.2961270	138318082.0	10094.23744			
9	17	66	14	39	0.883	300.4506045	-.4345370	89.9915872	59.2597752	138249540.2	10094.08315			
1	1	67	0	1	0.0	173.8268736	-25.4945481	90.0386195	107.3181848	138405674.9	10083.06873			

*M = Month, D = Day Y = Year, H = Hour. MI = Minute. S = Second.
Also, see notes at Bottom of Table A8

Table A8

Syncom Vector Elements as Reported by DOD, Air Force Systems Command

Syncom 3											
Date (U.T.)											
M	D	Y	H	MI	S	$\alpha°$	$\delta°$	$\beta°$	AZ°	RAD'	V/FPS
2	4	65	0	0	0	329.3087100	.672138	89.9941822	89.923047	138375573.3	10085.61611
3	5	65	0	0	0	337.2338772	.0907950	89.9957186	89.9519873	138387194.8	10085.00939
3	11	65	0	0	0	342.465331	.0930934	89.9927339	89.9545506	138387868.4	10084.73452
3	6	65	0	0	0	346.9072271	.3243960	90.0036182	90.040089	138442281.5	10081.23290
3	24	65	0	0	0	353.5587907	.0634430	89.9974880	90.0087157	138364442.3	10085.98775
3	31	65	0	0	0	-.0297323	-.0466264	89.9945489	90.0218809	138309091.8	10089.18472
3	31	65	0	0	0	225.6557090	-.0349054	90.0046737	89.9631400	138318082.0	10088.34542
7	8	65	5	11	0	173.8584686	.1177573	90.0007217	89.9671938	138333100.1	10087.65142
7	14	65	13	25	0	303.6761356	-.0573860	89.9978681	90.1236198	138335567.3	10087.64151
7	20	65	13	25	0	309.7154355	-.0620873	89.9971435	90.1190876	138336828.1	10087.21652
9	2	65	14	25	0.0	9.7560703	-.2697071	90.0000097	90.0123450	138335712.4	10087.11885
9	29	65	13	41	0.0	26.9170975	-.2961765	90.0012623	89.9495137	138334916.4	10087.08653
10	15	65	1	30	8.883	219.6767686	.2590034	89.9986513	90.0395497	138280569.8	10091.82446
11	11	65	0	1	14.875	222.2051107	.2747621	90.0001025	90.0741580	138312827.4	10090.10942
11	23	65	23	32	17.739	226.8336731	.2761059	90.0003455	90.1791327	138316354.7	10089.77591
12	9	65	23	25	6.427	239.7850209	.2948162	90.0039197	90.3207487	132315950.9	10089.68714
Corrected Orbit					(6.384)	(239.7821569)	(.2834610)	(90.0044185)	(90.3277418)	(138315042.5)	(10089.75657)
12	21	65	23	0	8.657	244.6624456	.2502542	90.0005093	90.3725080	138317347.2	10059.55986
	(22)	Cor. Orb.		(11)	(46.219)	(248.5289543)	(.2389576)	(90.0009380)	(90.3940341)	(138319005.7)	(10089.41514)
1	5	66	22	59	25.906	258.5706397	-.0085589	89.9936737	90.2325447	138287344.2	10091.68830
C. Orb.	(6)		(23)	(4)	(31.968)	(260.7895521)	(-.0158445)	(89.9935676)	(90.2373577)	(138288609.2)	(10091.57113)
1	19	66	20	56	16.662	240.8567046	.0717809	90.0022661	90.2796546	138295615.7	10090.89758
2	4	66	20	44	20.747	252.9875511	.2019325	90.0069535	90.5668549	138312648.7	10089.54462
3	3	66	22	1	14.254	298.0440906	-.2997467	90.0026493	90.6568832	138310811.7	10089.77604
3	17	66	22	34	35.662	319.8424334	-.5453541	90.0018012	90.56183511	138319644.1	10089.08818
3	30	66	21	24	23.764	314.7805399	-.5317386	89.9994567	90.5276043	138313388.1	10089.48471
4	10	66	0	13	2.374	6.7218328	-.7224497	90.0011987	89.9537090	138329513.3	10088.16882
5	2	66	23	28	43.618	17.9376586	-.7580983	90.0018212	89.8618606	138324944.6	10088.64166
5	17	66	0	1	44.652	39.8916786	-.7961832	89.9983801	89.4885543	138318036.3	10089.08628
6	1	66	0	56	32.305	68.2949586	-.4778375	89.9980245	89.1712197	138310369.7	10089.60206
6	20	66	1	8	18.168	89.6999357	-.0837705	89.9974096	89.0012170	138320870.1	10089.34540
6	30	66	23	51	25.402	80.6468849	-.2472802	90.0014671	89.0450739	138312020.7	10089.94653
7	14	66	17	37	40.716	0	-.9924101	90.0129977	90.1462207	138353051.0	10086.69946
9	16	66	18	5	32.019	67.8130270	-.6941001	90.0027906	88.9776683	138317331.3	10083.92757
10	14	66	11	45	58.370	0.0	-1.2705583	90.0089077	90.1510399	138337220.9	10087.68599
12	13	66	15	40	21.168	117.3088697	.5734308	89.9964678	88.6843516	138334769.4	10087.66824
1	1	67	0	1	0.0	260.3029154	.3491017	90.0037591	91.4563330	138340290.5	10087.30701

*The elements refer to the equinox and equator of date.
The earth model used to determine the elements, from data over about a week's duration (maximum), has the following parameters:

μ = .0053045314 E.R.^{3}/min^2
R_o = 20925738.19 FT/E.R.
I Km.= 3280.8399 Ft.

Zonal gravity field through J_8: Ref., W.H. Guier (1965), "Recent Progress in Satellite Geodesy" Applied Physics Lab. Report TG-659, Feb. 1965, Johns Hopkins Univ., Silver Spring, Maryland.

Non zonal gravity field through J_{44}: Ref. (Prior to spring 1966); W.H. Guier & R.R. Newton (1963), "Non Zonal Harmonic Coefficients of the Geopotential from Satellite Doppler Data", APL John's Hopkins Univ. Report # TG-520 (1963) Ref., (after spring 1966); Guier & Newton (1963) except for H_{22} and H_{33} Harmonics which are from C.A. Wagner (1966), "Longitude Variations of the Earth's Gravity Field as Sensed by the Drift of Three Synchronous Satellites", Journal of Geophys. Res., 71, #6, 1703 (1966).

Non zonal gravity field from J_{51} to J_{88}: Ref., W.H. Guier (1965), used after spring 1966.

Table A9

Syncom 2 Orbit Data in Arc 8 as Reported by DOD

Orbit Epoch (Yr-Mo-Day-Hr-Min-Sec, U.T.)	Time of Crossing (Day-Hr-Min-Sec)	R.A. of A.N. Deg's) *	H.A. of G at Cross. (Deg's) **	λ, Long. of Cross. (Deg's)	Long. Shift. of Cross. Over One Revolution (Deg's)	i, Inclination (Deg's)	Time of Crossing (Days From) 1965.0)	(Cross. Long. Difference) ΔL (Deg's)	(Drift Time) ΔT (Days)	Drift Rate ΔL/ΔT (°/Day)	Mean Long. (Deg's)
	Ascending Equator Crossing Data Nearest Orbit Epoch										
65-7-13-7-25-0	12.8643	(-52.487)	(241.682)	65.831	0.031	31.696	193.8643				
								.191	7.9771	.0239	65.93
65-7-21-2-56-0	20.8414	(-52.681)	(241.297)	66.022	0.034	31.638	201.8414				
65-7-28-7-26-0	27.8216	(.652)	(.049)	66.299	0.039	31.640	208.8216	.277	6.9802	.0397	66.16
65-8-4-2-56-0	3.8019	(.647)	(240.840)	66.513	0.040	31.665	215.8019	.214	6.9803	.0307	66.41
								.370	9.9740	.0371	66.70
65-8-13-19-55-0	13.7759	-52.920		66.883	0.050	31.634	225.7759				
								1.047	18.9415	.0553	67.41
65-9-2-3-25-0	1.7174	(-53.152)	(238.918)	67.930	0.056	31.583	244.7174				
								1.346	22.9328	.0587	68.60
65-9-25-2-56-0	24.6502			69.276	0.069	31.517	267.6502				
								1.283	19.9410	.0643	69.92
65-10-14-11-49-48	14.5912			70.559	0.070	31.442	287.5912				
								2.174	26.9187	.0808	71.65
65-11-10-9-58-5	10.5099			72.733	0.078	31.470	314.5099				
								.924	12.9639	.0713	73.20
65-11-23-9-11-46	23.4738	-54.551		73.657	0.077	31.433	327.4738				
								1.329	15.94914	.0833	74.32
65-12-9-8-17-6	9.42294	-54.812	230.202	74.986	0.077	31.404	343.42294				
								1.037	12.96106	.0800	75.50
65-12-22-7-28-43	22.3840	(-55.017)	(228.960)	76.023	0.080	31.376	356.38400				
								1.129	14.9556	.0755	76.59
66-1-6-6-42-18	6.3396	-55.105		77.152	0.079	31.288	371.3396				
								1.128	13.95809	.0808	77.72
66-1-20-6-19-13	20.29769	-55.334	226.386	78.280	0.079	31.276	385.29769				
								1.014	13.95855	.0726	78.79
66-2-4-5-26-15	3.25624	-55.481	225.223	79.294	0.074	31.175	399.25624				
								2.158	27.92266	.0773	80.37
66-3-4-3-39-42	3.1789			81.452	0.070	31.186	427.1789				
								.929	13.9527	.0666	81.92
66-3-18-2-35-48	17.13160	-55.997	221.627	82.381	0.064	31.141	441.13160				
						Avg: 31.4 = i					
						Avg: 6.61 = a					

*Right ascension of the ascending node: **Hour angle of Greenwich: ( ) = Estimated, not reported, data

Table A10

Syncom 3 Orbit Data in Arc 11 as Reported by DOD

Orbit Epoch (Yr-Mo-Day-Hr-Min-Sec., U.T.)	Ascending Equator Crossing Data Nearest Orbit Epoch					
	Time of Crossing (Day)	λ, Longitude of Crossing (Deg's)	Longitude Shift of Crossing in One Revolution (Deg's)	i, Inclination (Deg's)	Time From Nov. O.O, 1965 (Days)	Time From Nov. 75.0, 1965 (Days)
65-11-12-0-3-51	11.6705	171.914	-0.0775	0.384	11.6705	-63.3295
65-11-23-23-32-18	23.6445	171.115	-0.701	0.329	23,6445	-51.3555
65-12-9-23-25-6	9.5952	170.042	-0.0615	0.433	39.5952	-35.4048
65-12-22-23-11-46	22.5534	169.313	-0.053	0.460	52.5534	-22.4466
65-1-6-23-4-32	6.4545	168.606	-0.455	0.237	67.4545	-7.5455
66-1-19-20-56-17	19.4123	167.997	-0.042	0.288	80.4123	5.4123
66-2-4-20-44-21	4.4193	167.401	-0.038	0.602	96.4193	21.4193
66-3-3-22-1-14	3.3506	166.543	-0.029	0.721	123.3506	48.3506
66-3-17-22-34-36	17.3194	166.180	-0.024	0.782	137.3194	62.3194
				Avg: 0.53 = i		
				Avg: 6.61 = a		

Table A11

Syncom 3 Orbit Data in Arc 13, as Reported by DOD

Date	Longitude of Asc. Eq. Cross (Deg's)	Time From 6 Sept. 1966 (Days)	$\dot{\lambda}$, Observed From Eq. Cross. Long. Shift in One Revolution (Deg./Day)	$\dot{\lambda}$, Calculated From Long Term Long. Drift (Deg./Day)
8 Sept. 1966	161.28	2	-0.005	
	(161.245)	(5.5)		(-0.010)
15 Sept. 1966	161.21	9	-0.010	
	(161.15)	(16)		(-0.0085)
29 Sept. 1966	161.09	23	-0.009	
	(161.02)	(30.5)		(-0.0095)
14 Oct. 1966	160.95	38	-0.013	
	(160.655)	(60)		(-0.010)
13 Dec. 1966	160.36	98	-0.012	
	(160.275)	(105)		(-0.012)
27 Dec. 1966	160.19	112	-0.012	
	(160.065)	(119.5)		(-0.0165)
11 Jan. 1967	159.94	127	-0.016	

Table A12

Equator Crossing Data and Sets of Elements for Early Bird in Arcs 9 and 12

Date: Yr-Mo-Day	Time (Hr)	Ascending Equator Crossing Longitude (Deg's West)
65-4-23	15.8	30.005
24	16	29.945
26		.835
27		.780
28		.720
29		.670
30		.625
5-1	15	.570
2		.530
4		.425
5		.375
6		.325
7		.285
8		.245
10		.165
11		.115
12		.075
13		.045
14		.000
15		28.960
16		.925
18	14	.850
19		.815
20		.780
21		.740
22		.705
23		.670
24		.640
25		.605
26		.580
27		.555
28		.530
29		.505
30		.480
31		.455
6-1		.430
2		.405
3		.385
6		.310
7		.295
8	13	.275

Date	Time (Hr)	A.E.C. Long.	Time (Hr)	Descending Equator Crossing Longitude (Deg's West)
65-6-9	13	28.255		
14		.185		
17		.140		
19		.125		
21		.105		
22	12.65	.084		
23	12.5	.075		
24		.074		
26		.078		
27		.056		
28	12.25	.054		
29		.036	25.9	28.057
30		.064		
7-1		.054		.073
2		.041		.070
3		.096		.158
4		.116		.162
5		.043		.089
6		.108		.160
7		.064		.100
8		.094		.141
9		.058		.142
10		.115		.118
11		.120		.142
12		.100		.115
13	11.5	.110		.127
14		.105		.144
15		.110		.160
16		.140		.172
19		.200		
20		.202		
21		.219		.255
22		.312		.319
23		.308		.331
24		.317		.347
25		.336		.360
26		.367		.391
27		.376		.415
28		.402		.438
29		.418		.469
30		.441		.486

Date	Time (Hr)	A.E.C. Long.	Time (Hr)	D.E.C. Long.
65-7-31		28.471		28.513
8-1		.453		.531
2		.451		.566
3		.510		.585
4		.539		.564
5		.563		.602
6		.607		.650
7		.639		.674
8		.669		.700
9		.705		.734
10		.736		.769
11				.794
12		.809		.835
13		.844		.868
14				.903
15		.922		.947
16		.952		.984
17		.991		29.023
18		29.052		.069
19		.073		.115
20		.120		.149
21		.158		.197
22		.199		.243
23		.257		.280
24		.280		.333
25		.338		.387
26		.382		.427
27		.432		.484
28		.485		.535
29		.527		.582
30		.586		.629
31		.633		.686
9-1			22	.758
2				.792
3				.846
4				.901
5				.950
6				30.006
7				.070
8				.117
9			21.5	.181

Table A12 (Cont.)

Equator Crossing Data and Sets of Elements for Early Bird in Arcs 9 and 12

Date	Time (Hr)	A.E.C. Long.	Time (Hr)	D.E.C. Long.
65-9-10				30.257
18				.790
19				.860
20				.932
21				31.004
23				.144
24				.239
27				.476
28				.555
30				.714
10-2				.863
3				.951
4	7	31.960		32.036
5		32.026	20	.112
6		.115		.198
7		.198		
8		.285		.369
9		.379		
10		.471		.550
11	6.5	.565		.643
12		.658	19.6	.734
13		.753		.830
14		.844		.920
15		.935		33.019
16		33.026		.115
17		.128		.211
18		.230	19	.312
19		.327		.411
20		.430		.516
21	6	.525		.614
22		.638		.723
23		.736		.820
24		.843		.923
25		.955		34.037
26		34.061		.142
27	5.5	.166		.249
28		.280		.359
29		.381		.464
30		.489		.572
31		.599		.685
11-1		.711	18.3	.797

Date	Time (Hr)	A.E.C. Long.	Time (Hr)	D.E.C. Long.
65-11-2			18.2	34.906
3				35.021
4				.137
5				.251
6				.368
7				.494
8	5.0	35.535	18.0	.617
9				.739
10				.862
11				.988
12				36.109
13				.239
14				.357
15				.487
16				.620
17				.750
18				.884
19				37.015
20				.146
21				.285
22				.416
23				.555
24				.689
25				.824
26				.964
27				38.115
28				.248
29				.394
12-1				.794
	← Orbit Maneuver →			
2	3.9	38.725	16.3	38.596
3		.585		.457
4		.446		.318
5	3.8	.306		.179
6	3.7	.170		.039
7	3.6	.033		37.907
8	3.5	37.895		.769
9	3.4	.761		.637
10		.624		.500
11	3.3	.491		.367
12	3.2	.335		
13		.229		.110

Date	Time (Hr)	A.E.C. Long.	Time (Hr)	D.E.C. Long
65-12-14	3.1	37.099		36.978
15	3.0	36.970		.849
16	2.9	36.839		.725
17		.719		.610
18		.593		
19		.471		.357
20	2.7	.339		
21		.201		.079
22	2.5	.088		35.986
23		35.962		.860
24	2.3	.835	14.5	.738
25		.714		.620
26		.597		.501
27		.476		.382
28		.360		.264
29		.252		.158
30		.139		.047
31				34.937
66-1-1				.827
2				.722
3				.623
4				.510
5				.400
6				.305
7				.197
8				.101
9				.911
10		33.873		33.907
11		.776	13.2	.805
12		.678		.711
13		.588		.621
14		.493		.519
15		.398		.426
16		.304		.334
17		.209		.239
18		.123		.147
19		.027		.059
20		.937		32.967
21		.845		.875
22		.760		.790
23		.677		.700

Date	Time (Hr)	A.E.C. Long.	Time (Hr)	D.E.C. Long.
66-1-24		32.585		32.618
27		.343		.369
28		.268		.295
29		.183		.217
30		.104		.151
31		.027		.057
2-1		31.943		31.988
2		.864		.898
3		.788		.812
4		.708		
5		.636		.670
6		.567		.611
7		.493		.527
8		.427		.465
9		.359		.391
10		.291		.326
11		.227		.264
12		.161		.193
13		.104		.113
14		.037		.059
15		30.967		30.989
16		.910		.930
17		.839		.868
18		.776		.808
19		.715		.742
20		.657		.683
21		.599		.627
22		.542		.570
23		.487		.513
24		.431		.460
25		.397		.404
26		.323		.351
27		.268		.299
28		.216		.246
3-1		.167		.209
2		.117		.133
3		.066		.096
4		.019		.044
5		29.973		.000
6		.933		29.955
7		.855		.914

Table A12 (Cont.)

Equator Crossing Data and Sets of Elements for Early Bird in Arcs 9 and 12

Date	Time (Hr)	A.E.C. Long.	Time (Hr)	D.E.C. Long.	Date	Time (Hr)	A.E.C. Long.
66-3-8		29.839		29.874	66-4-18		28.783
9		.796		.830	19		.770
10		.757		.795	20		.768
11		.720		.757	21		.764
12		.679		.707	22		.757
13		.639		.674	23		.754
14		.598		.625	24		.758
15		.561		.585	25		.751
16		.521		.548	26		.743
17				.510	27		.739
18		.450		.482	28		.744
19		.417		.438	29		.739
20		.382		.403	30		.743
21		.352		.372			
22		.317		.340	5-1		.750
23		.289		.304	2	17.25	.756
24		.264		.272	3		.758
25		.232		.242	4	17.0	.770
26		.203		.221	5		.767
27		.171		.193	6		.776
28		.147		.159	7		.783
29		.118		.141	8		.790
30		.094		.115	9		.799
31		.071		.091	10		.808
					11		.815
4-1		.045		.069	12		.823
2		.025			13		.840
3		.005		.038	14		.848
4		28.985					
5		.968		28.988			
6		.954		.979			
7		.936		.963			
8				.950			
9		.901					
10		.886					
11		.874					
12		.859					
13		.842					
14		.832					
15		.815					
16		.805					
17		.794					

Keplerian Vector Elements*

Date Yr-Mo-Day-Hr-Min-Sec, U.T.	a (Earth Radii)	i (Deg's)	ω (Deg's)	e	β (Deg's)	M.A. (Deg's)
65-5-17-0-0-0.000	6.610564	.185	320.886	349	82.630	162.080
65-6-7-0-0-0.000	6.610548	.261	324.945	425	77.923	184.005
65-6-21-13-6-0.000	6.610900	.332	328.992	330	76.785	32.162
65-7-1-0-0-0.000	6.610900	.332	329.246	330	76.658	204.923
65-7-6-0-0-0.000	6.610950	0.332	329.380	0.000330	86.591	199.727
65-7-12-12-28-0.000	6.611232	.241	348.634	428	103.894	356.565
65-8-24-9-52-0.130	6.611568	0.473	335.833	0.000337	93.571	21.706
65-9-2-12-59-29.990	6.610640	0.520	339.964	0.000377	93.487	73.053
10-3-20-1-15.000	2078	.562	331.807	202	96.506	212.332
10-25-12-4-0.000	6.612301	.591	346.019	228	96.216	98.402
11-15-14-5-0.000	6.612642	.602	334.349	146	92.283	162.571
← Orbit Maneuver (65-12-2-1-20) →						
65-12-2-1-24-0.000	6.609187	.671	149.533	383	90.717	172.674
12-2-1-24-0.000	6.609171	.646	145.430	322	90.204	177.298
65-12-30-14-2-0.000	6.609548	.762	154.333	375	90.689	29.173
66-2-4-0-10-0.000	6.610260	.870	151.977	295	92.079	220.333
3-10-21-1-0.000	384	.936	178.188	264	93.275	182.069
66-4-4-9-40-0.000	618	.984	213.985	138	93.311	0.938

*These are all osculating elements: a = semimajor axis, i = inclination, ω = argument of perigee, e = eccentricity, β = right ascension of the ascending node, M.A. = mean anomaly. The earth constants used in the orbit determination were: $\mu = 3.96801 \times 10^5\ km^3/sec^2$, R_O = 6378.155 km/earth radii, $J_2 = 1082.6 \times 10^{-6}$. i and β refer to the equator and equinox of date.

APPENDIX B
Estimating the Harmonic Variability

From the covariance statistics, derived as a by-product of the least squares fitting process, we can estimate the degree of harmonic variability which the data allows. In this calculation, the model is assumed to be unbiased with respect to the data. The data residuals are assumed to be uncorrelated and random normally distributed. In addition, the measurement variances are assumed to produce realistic weights for the data in those model tests where weighting is employed. Actually, we know the abbreviated models tested cannot yield unbiased residuals with this limited data, or uncorrelated residuals, due to the effects of the harmonics ignored in the fit. Nevertheless, we can hope to learn something of the variability in the abbreviated model, allowed by the data, if we proceed in two stages. In the first stage, we assume that all the unmodeled effects are zero. If this were the case, our assumptions as to unbiasness, noncorrelation and realistic weights would be true. In the second stage of assessing the modeled harmonics variability, we can actually account for the unmodeled effects by using likely values for them from outside sources. If these outside-source values are reasonably realistic, then again the residuals should be unbiased and uncorrelated, and the statistics of the solution would be valid.

In this report, the covariance statistics are chosen from the solution without any assumption as to unmodeled effects (Solution 6, Table 2; also see Figure 2). (The general least squares program used, and the derivation of the statistical data from it, is described in Reference [B1].) In this way, we maintain maximum faithfulness to the actual data; for example, in the determination of accelerations of <u>new</u> 24 hour satellites, and in comparison of the results with other determinations from different data. However, we acknowledge the likely contribution of unmodeled effects by observing the gross changes possible in the modeled harmonics, when reasonable values for these effects are included in least squares solutions. This second stage process has been described already in the text. The best harmonic solution (at the bottom of Table 2) has bounds which are set by considering both the internal variability of the solution (first stage error analysis) and the variability of the harmonics themselves in tests with reasonable account taken of unmodeled, higher order resonance effects.

A more desirable and logical way to conduct the first stage error analysis (no <u>specific</u> assumptions on higher order terms) would be to increase all the data deviations by an expected RMS (root mean square) deviation due to the unmodeled effects. While this would not eliminate the bias and correlation of the residuals in the first stage analyses, it would result in more realistic weights to the data and a better overall solution. For example, Reference [4] shows that the unmodeled 4th order harmonics may produce accelerations as high as $.016 \times 10^{-5}$ radians/day ^{2} (H_{44}) and $.018 \times 10^{-5}$ rad./day ^{2} (H_{42}) on the geostationary satellite. In gravity solutions only for H_{22}, H_{31} and H_{33}, an expected data deviation (RMS), due to H_{42} and H_{44}, of $.707\ (.016^2 + .018^2)^{1/2} \times 10^{-5} = .017 \times 10^{-5}$ rad/day ^{2} should be allowed for in the measurements on the geostationary satellites. Measurements on the moderately inclined Syncom 2 in this limited model test need allow for only $.009 \times 10^{-5}$ rad/day ^{2} RMS deviation due to H_{42} and H_{44}, principally because the effect of H_{42} is almost negligible at the inclination of that satellite. Future 24 hour satellite limited gravity tests will be made with increased data variance to achieve better overall solutions.

1σ Ellipses

The 1σ ellipses in Figure 2 summarize the covariance statistics of the basic (six parameter, three gravity term) solution (first stage error analysis) as it applies to the permitted variability of each harmonic term as seen by the data. Each harmonic term is specified by the coefficients $C_{\ell m}$ and $S_{\ell m}$, so that the statistics necessary to define its variability are:

$$\tilde{C}_{\ell m},\ \tilde{S}_{\ell m},\ \sigma C_{\ell m},\ \sigma S_{\ell m} \text{ and } c\,(C_{\ell m},\ S_{\ell m});$$

the first two symbols being the least squares estimates of the harmonic coefficients, the second two, their standard deviations and the last, the correlation coefficient ($-1 < c < 1$). Providing the experiment residuals are random normally distributed, it is shown in Reference [B2] that the above statistics define a probability ellipse, λ, in the $C_{\ell m}, S_{\ell m}$ plane defined by:

$$\frac{(C_{\ell m} - \tilde{C}_{\ell m})^2}{(\sigma C_{\ell m})^2} - \frac{2c\,(C_{\ell m} - \tilde{C}_{\ell m})\,(S_{\ell m} - \tilde{S}_{\ell m})}{(\sigma C_{\ell m})\,(\sigma S_{\ell m})}$$

$$+ \frac{(S_{\ell m} - \tilde{S}_{\ell m})^2}{(\sigma S_{\ell m})^2} = \gamma^2 . \qquad \text{(B1)}$$

This ellipse has the property that on it, the probability density function for possible sets of C_{ℓ_m} and S_{ℓ_m} seen by the data, is constant. The ellipse scale is set by γ^2 which defines the probability $P(\gamma)$ of finding sets of C_{ℓ_m} and S_{ℓ_m} within the ellipse. It is shown in Reference [B2] by a simple integration of the density function that this probability $P(\gamma)$ is related to γ^2 and c by the formula:

$$P(\gamma) = 1 - \exp\left[-\gamma^2/2(1-c^2)\right]. \tag{B2}$$

Thus, for example, the 1σ probability ellipse contains an area in which it is expected that 68.26% of the sets of C_{ℓ_m} and S_{ℓ_m} values will fall. Evaluating (B2) for $P(\gamma) = 0.6826$,

$$\gamma^2_{1\sigma} = 2.30\,(1-c^2). \tag{B3}$$

Similarly, the 2σ ellipse $[P(\gamma) = .9544]$ defines the scale size from:

$$\gamma^2_{2\sigma} = 6.16\,(1-c^2) \tag{B4}$$

A rather simple exercise in analytic geometry shows that the probability ellipse of Equation (B1), with respect to the C_{ℓ_m}, S_{ℓ_m} plane:

1) Is centered at $\tilde{C}_{\ell_m}$, $\tilde{S}_{\ell_m}$,

2) Has major (A) and Minor (B) axes given by:

$$A = 2\gamma^2/\{D - [E^2 + 4c^2/F^2]^{1/2}\} \tag{B5}$$

$$B = 2\gamma^2/\{D + [E^2 + 4c^2/F^2]\} \tag{B6}$$

where

$$D = \frac{1}{(\sigma C_{\ell_m})^2} + \frac{1}{(\sigma S_{\ell_m})^2}$$

$$E = \frac{1}{(\sigma C_{\ell_m})^2} - \frac{1}{(\sigma S_{\ell_m})^2} \tag{B7}$$

and

$$F = (\sigma C_{\ell_m})(\sigma S_{\ell_m}),$$

and

3) Has it's <u>minor</u> axis (B) rotated counterclockwise from the C_{ℓ_m} axis by an angle θ, given by:

$$\theta = \frac{1}{2} \mathrm{TAN}^{-1} \frac{-2c/F}{E} \tag{B8}$$

These formulas have been used in constructing the probability ellipses in Figure 2 from the covariance statistics of the basic solution (6) in Table 2.

After considering the likely model bias effects (in the second stage of the error analysis) on the basic solution, somewhat subjective upper and lower <u>realistic</u> bounds have been set on the modeled coefficients. They are displayed by the dashed boxes in Figure 2. Defining the absolute variability possible in H_{ℓ_m} by the boxed bounds, does not take into account the correlation between C_{ℓ_m} and S_{ℓ_m} in the various tests used to set these bounds. Therefore, the boxed bounds for H_{ℓ_m} should be reasonably conservative since the set of C_{ℓ_m}, S_{ℓ_m} values used to define it do not (in general) tend to fill the inner space in a random manner. To insure this conservatism in reporting the J_{ℓ_m} and $m\lambda_{\ell_m}$ coefficients (which are the polar coordinates of points in the C_{ℓ_m} and S_{ℓ_m} plane), I have calculated the possible extremes of their variation by considering rays to the corners of the boxed bounds in Figure 2. In future reports, the correlation of coefficient solutions will be taken into account when the unmodeled effects are estimated. When this is done, the absolute bounds on the gravity solution should be known more precisely.

<u>References:</u>

B1. Kunin, M. J., "Snap-7090 Multiple Regression Analysis Program," IBM 7090 Program No. 183, "SHARE" distribution number 1289, New York: Shell Oil Company Data Processing Dept., Shell Oil Company, 111 West 50th St., New York, N. Y. (1962).

B2. Shchigolev, B. M., "Mathematical Analysis of Observations," Pub: London, Iliffe Books Ltd; New York, American Elsevier Publishing Company, Inc.

APPENDIX C
List of Symbols

$J_{\ell m}$, $\lambda_{\ell m}$: Specifying the amplitude ($J_{\ell m}$) and phase angle ($\lambda_{\ell m}$) of the spherical gravitational harmonic $H_{\ell m}$ whose order (or latitude frequency) is ℓ and whose longitude frequency is m.

$H_{\ell m}$: Referring to the spherical gravitational harmonic of order ℓ and longitude frequency m .

$\dot{x}$, $\ddot{x}$: $\frac{dx}{dt}$, $\frac{d^2x}{dt^2}$

a , a_s : Semimajor axis of the satellite's orbit, synchronous semimajor axis (a_s = 6.611 earth radii).

i : Inclination of the satellite's orbit.

σ: Standard deviation.

ΔV: Velocity increment.

γ: Parameter defining the scale of the probability ellipse.

c : Correlation coefficient.

E.R. : Earth radii.

RMS : Root mean square.

A.E.C. : Ascending equator crossing.

D.E.C. : Descending equator crossing.